Interaction Notes

Note 360

October 1978

Extrapolation of Induced Transient Surface Currents on a Scatterer to General Band-Limited Excitation Conditions

L. Wilson Pearson
D. Randall Roberson

University of Kentucky
Lexington, KY 40506

Abstract

A technique for the extraction of an approximate singularity expansion description of the electromagnetic response of a scatterer is presented. The description is extracted from transient waveforms which are spatial samples of the transient current on the scatterer excited by a known excitation. The method can use any reliable Prony-type processor for exponential analysis of the transient waveforms so long as it provides physically-meaningful poles from the waveforms. The fact that singularity expansion poles are common to all waveforms on the object provides a computational advantage over a waveform-by-waveform Prony-type analysis. A "consensus pole set" procedure is described to exploit this redundancy. Some issues relating to the completeness of a set of transient data to the class of excitations to which the singularity expansion is applied is discussed. The one-dimensional example of a thin-wire scatterer is used to test the practicability of the method. The ultimate utility of the method is demonstrated by way of expansion of the extracted data to new excitations. Recommendations are made toward an implementation of the method using measured data.

Acknowledgement

This work was sponsored by the Office of Naval Research, Arlington, VA

Interaction Notes

Note 360

October 1978

Extrapolation of Induced Transient Surface Currents on a Scatterer to General Band-Limited Excitation Conditions

L. Wilson Pearson
D. Randall Roberson

University of Kentucky
Lexington, KY 40506

Abstract

A technique for the extraction of an approximate singularity expansion description of the electromagnetic response of a scatterer is presented. The description is extracted from transient waveforms which are spatial samples of the transient current on the scatterer excited by a known excitation. The method can use any reliable Prony-type processor for exponential analysis of the transient waveforms so long as it provides physically-meaningful poles from the waveforms. The fact that singularity expansion poles are common to all waveforms on the object provides a computational advantage over a waveform-by-waveform Prony-type analysis. A "consensus pole set" procedure is described to exploit this redundancy. Some issues relating to the completeness of a set of transient data to the class of excitations to which the singularity expansion is applied is discussed. The one-dimensional example of a thin-wire scatterer is used to test the practicability of the method. The ultimate utility of the method is demonstrated by way of expansion of the extracted data to new excitations. Recommendations are made toward an implementation of the method using measured data.

Acknowledgement

This work was sponsored by the Office of Naval Research, Arlington, VA

TABLE OF CONTENTS

Chapter		Page
I.	INTRODUCTION	6
	SEM Description of a System	6
	Prony-type Data Analysis as Motivated by SEM	7
	The Contribution of Present Work	8
II.	DESCRIPTION OF THE TRANSIENT EXTRACTION METHOD	9
	Description	9
	Signal Processing Considerations	14
	Data Completeness Considerations	16
III.	EXTRACTED SEM RESULTS	20
	Introduction	20
	The Influence of the Spectrum of the Excitation of Recoverable Poles	22
	Extracted SEM Parameters - Even Mode Case	25
	Extracted SEM Parameters - General Case	29
IV.	EXTRAPOLATED RESULTS	42
	Introduction	42
	Gaussian Plane Wave Excitation	42
	Reexpansion for Double Exponential Excitation	47
V.	CONCLUSIONS	51
REFERENCES		53

LIST OF FIGURES

Figure Page

1. Pictorial representation of spatial current density sampling vectors on the surface of a scatterer. 10

2. Groupings of poles which occur in obtaining the consensus pole set. 15

3. Mode 2 of a thin cylindrical scatterer which does not couple for the center excitation shown. 17

4. (a). TWTD model of the wire scatterer with the generator at the center segment: zone 25.
(b). Model of the Gaussian generator used for excitation, showing the "waist" parameter. 21

5. The spectrum of the Gaussian forcing function, with a waist of 0.6158 nanoseconds, shown with the poles extracted from the transient response it generated: Example 1. 23

6. The spectrum of the Gaussian forcing function, with a waist of 0.3077 nanoseconds, shown with the poles extracted from the transient response it generated: Example 2. 24

7. Real and imaginary parts of modes 1 and 7 obtained from the transient data of Example 1. 27

8. Real and imaginary parts of mode 9 obtained from the transient data of Example 1 compared with that of Tesche. 28

9. Real and imaginary parts of modes 1, 3, and 5 derived from the transient data of Example 2. 30

10. Real and imaginary parts of modes 7 and 9 derived from the transient data of Example 2. 31

11. Real and imaginary parts of modes 11 and 13 derived from the transient data of Example 2. 32

12. Real and imaginary parts of modes 15 and 17 derived from the transient data of Example 2. 33

13. Real and imaginary parts of mode 1 derived from the transient data of Examples 3 and 4: off center excitation. 37

14. Real and imaginary parts of mode 2 derived from the transient data of Examples 3 and 4: off center excitation. 38

15. Real and imaginary parts of mode 5 derived from the transient data of Examples 3 and 4. 39

16. Transient currents for a plane wave with a Gaussian time history at 0 degrees incidence. 42

17. Transient currents for a plane wave with a Gaussian time history at 30 degrees incidence. 45

18. Transient currents for a plane wave with a Gaussian time history at 60 degrees incidence. 46

19. Transient currents for a plane wave with a double exponential time history at 0 degrees incidence. 48

20. Transient currents for a plane wave with a double exponential time history at 30 degrees incidence. 49

21. Transient currents for a plane wave with a double exponential time history at 60 degrees incidence. 50

LIST OF TABLES

Table		Page
1.	Consensus Poles and Those Reported by Tesche	26
2.	Transient Extracted Normalization Constants and Those Reported by Tesche	34
3.	Consensus Poles and Those Reported by Tesche	36
4.	Transient Extracted Normalization Constants and Those Reported by Tesche	41

CHAPTER I

INTRODUCTION

1.1 SEM Description of a System

The insight that the general transient response of a scatterer resembles a sum of exponentially damped sinusoids, led to the development of the Singularity Expansion Method (SEM) by Baum in 1971 [1,2]. The Singularity Expansion Method has since become a viable procedure for solving for the transient scattering from electromagnetic systems in the terms of the complex resonant frequencies of the structure. A collection of SEM parameters for a given scatterer include the complex resonances along with the associated modal current distributions and normalization coefficients. It is possible to expand this set of SEM parameters into a transient response for the given object under excitation conditions limited only by the extent of the parameter set.

To date, several open questions concerning the SEM representation have lingered. In particular,

- Of the several coupling coefficient forms postulated, which are valid?
- Must we, in general, include a contribution to the transient response which results from an entire function in the Laplace transform domain?
- How do the issues relating to the entire function contributions and coupling coefficient forms interact?
- What means exist to determine the SEM description for a scatterer

whose geometry is too complex to admit to analytical solution?

The first three of these questions are presently under investigation. The present work is an effort to provide a means of addressing the fourth.

1.2 Prony-Type Data Analysis as Motivated by SEM

Until recently the only method by which the SEM parameters were obtained for a structure was by using analytical/numerical methods such as integro-differential equations or boundary value techniques. This is practical for simple object geometries, but for a complex shaped object such as an aircraft, these approaches are impractical. The computational difficulty for the method is overwhelming for complex shapes. Therefore, techniques to efficiently extract the SEM parameters from experimentally derived data are sought.

The extraction of SEM poles and residues of a system from its transient response was first suggested by Mittra and Van Blaricum [3] and extensively elaborated upon by them [4,5]. The development of a least-squares Prony procedure by Van Blaricum and Mittra [6] gave a method to obtain these poles and residues from the transient response of the scatterer. Though the least-squares Prony procedure is computationally elegant and reliable, Dudley [7] has shown it introduces a bias in the estimate of the real part of SEM poles when noise is present in the transient data.

An alternative technique to extract the SEM poles and residues from transient responses in the presence of noise using a Prony-related procedure has been given by Lager, et al. [8]. This technique is the so-called "sliding-window Prony" procedure. Work by others to find a pole extractor tolerant of noise continues, but for the present work, only the application of existing pole extraction techniques has been consid-

ered. For the reader interested in the current developments of alternative methods, Van Blaricum has compiled an excellent bibliography [9]. A review paper on Prony-type analysis as applied to electromagnetic scattering problems appeared recently in the IEEE Transactions [10].

1.3 The Contribution of Present Work

This document reports the results of an effort to develop a procedure to extract the SEM description from a transient data. Chapter 2 presents the method used to derive the SEM description from spatially-sampled transient data. Signal processing and data completeness considerations are also discussed there. Chapter 3 reports the SEM parameters which have been extracted from transient data for several numerical examples. The relationship between recoverable SEM data and the frequency spectrum of the excitation are discussed there. Some results obtained from extrapolating these extracted SEM descriptions to new excitation conditions are given in Chapter 4. Chapter 5 presents conclusions drawn from the present study and suggests directions which future work in this area might take.

CHAPTER II

DESCRIPTION OF THE TRANSIENT EXTRACTION METHOD

2.1 Description

In this chapter we develop a method whereby an approximate SEM description for a given scatterer may be derived from spatial samples of transient currents excited on the scatterer.

Figure 1 pictures a scatterer with unit vectors $\hat{p}_j$ symbolically indicating current sample locations and orientation. A known incident field $\bar{E}^{inc}(\bar{r},t)$ excites a transient current $\bar{J}(\bar{r},t)$ on the object. The vector $\bar{r}$ indicates the spatial independent variable and t the time variable. Sampled current responses at the sites $\hat{p}_j$ are scalar functions of time of the form

$$r_j(t) = \hat{p}_j \cdot \bar{J}(\bar{r}_j,t). \tag{1}$$

The SEM description for the currents on the object can be written as

$$\bar{J}(\bar{r},t) = \sum_i \beta_i \, \eta_i^{(2)}(t) \, \tilde{f}(s_i) \, \bar{J}_i(\bar{r}) \, e^{s_i t} \tag{2}$$

where the β_i's are termed "normalization constants," $\tilde{f}(s_i)$ is the Laplace transform of the forcing function, $\bar{J}_i(\bar{r})$ is a "natural mode" vector and contains the spatial distribution information associated with a given pole, the s_i's are the complex natural frequencies or "poles", and $\eta_i^{(2)}(t)$ are the "Class 2 coupling coefficients" and are a measure of how much of a mode is contained in the current response for a given incident wave.

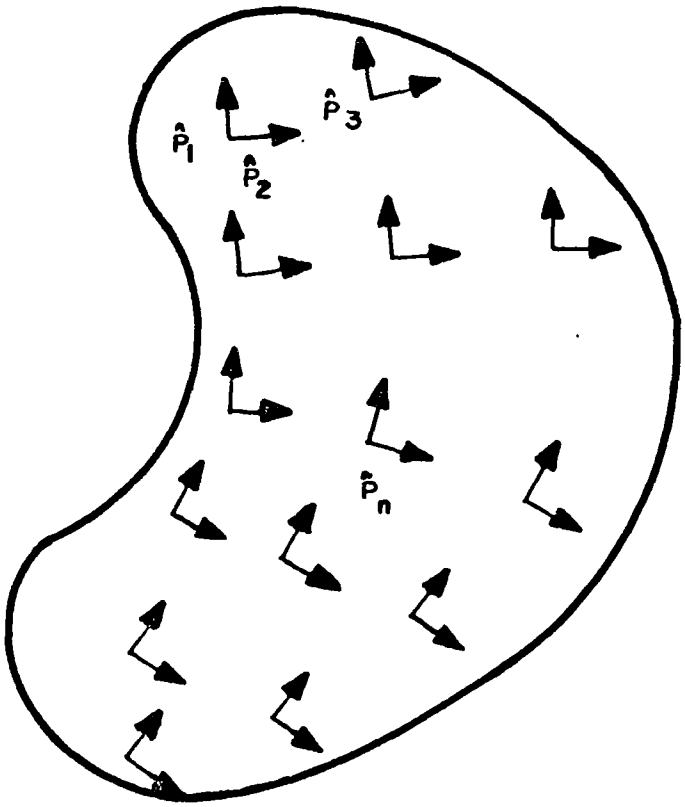

Figure 1. Pictorial representation of spatial current density sampling vectors on the surface of a scatterer.

The Class 2 coupling coefficient form [1,11] is chosen and no entire function contribution is included in the representation (2). It has been conjectured that the Class 2 coupling coefficient yields a zero entire function [12]. (It is pointed out that the present work does not depend on the validity of this conjecture.) After the leading edge of the incident field has passed over the structure, i.e. $t > T_c$, the Class 2 coupling coefficient becomes equal to the Class 1 coupling coefficient, which is a constant with respect to time. Hence we observe that for $t > T_c$, (2) admits to an exact temporal representation in terms of decaying exponentials.

If the sampling process indicated in (1) is applied to the SEM representation for the current given by (2) the result is

$$r_j(t) = \sum_i \beta_i \, \eta_i^{(2)}(t) \, \tilde{f}(s_i) \, \hat{p}_j \cdot \bar{J}_i(\bar{r}_j) \, e^{s_i t} \tag{3}$$

For time after the leading edge of the incident wave has passed over the structure, i.e. $t > T_c$, the Class 2 coefficients are equal to the Class 1 coefficients and the sampled currents take the form of a sum of decaying exponentials with constant coefficients:

$$\eta_i^{(2)}(t) = \text{const.} = \eta_i^{(1)}, \quad t > T_c, \tag{4}$$

and

$$r_j(t) = \sum_i A_{ij} \, e^{s_i t} \tag{5}$$

where

$$A_{ij} = \beta_i \, \eta_i^{(1)} \, \tilde{f}(s_i) \, \hat{p}_j \cdot \bar{J}_i(\bar{r}_j). \tag{6}$$

From here forward we adopt the common SEM/Prony vernacular and term the

A_{ij}'s "residues" and the s_i's "poles". This terminology is based on the role of these constants in the Laplace transform domain. Observe $r_j(t)$ are sampled currents which are real functions. Therefore, A_{ij}'s and s_i's must occur in complex conjugate pairs or lie on the real axis.

The key to the extraction procedure is the recognition that a function of the form (5) can be decomposed into its pole/residue components by means of Prony-type analysis [6]. Suppose we have available noise-corrupted observations $r_j^o(t)$ of the $r_j(t)$ signals. A Prony-type analysis approximates the corrupt signals as

$$r_j^o(t) \cong \sum_i A_{ij}^o \, e^{s_{ij}^o t} \tag{7}$$

where the A_{ij} and s_{ij}^o are the output of a Prony-type process applied to $r_j^o(t)$. The superscript "o" is used to indicate "observed" values.

In order to determine the SEM description from these data, we must match A_{ij}^o and s_{ij}^o with A_{ij} and s_i from equation (5). From equation (2) we see the poles of a system are independent of sample location j. If the observed data and the processing thereof were perfect this result would be evidenced by $s_{ij}^o = s_{ik}^o$ for all j,k. Because of the noise in both the data and the computer processing this result is not achievable. The next section describes a process which provides a single concensus extracted pole set for each set of spatial samples. This concensus pole set represents the first of the extracted SEM quantities.

The remaining SEM quantities are imbedded in the A_{ij}'s. From (6) we write in terms of "observed" SEM quantities

$$\beta_i^o \, \eta_i^{(1)^o} \tilde{f}(s_i) \, \hat{p}_j \cdot \overline{J}_i^o(\overline{r}_j) = A_{ij}^o. \tag{8}$$

The observation that the first three terms on the left-hand side are

constant with respect to the spatial variables leads to the conclusion that the left-hand side is a scaled natural mode. Thus we construct

$$\bar{J}_i^I(\bar{r}) = C_i \; I \{A_{i1}\hat{p}_1, A_{i2}\hat{p}_2, \ldots, A_{im}\hat{p}_m\} \tag{9}$$

where I is an interpolation operator and C_i a scale factor which is chosen to yield a sensible normalization of $\bar{J}_i^I(\bar{r})$.

With this approximate knowledge of $\bar{J}_i$ an approximation to the coupling coefficient is

$$\eta_i^{(1)o} = \iint_{\text{object}} \tilde{\bar{\bar{E}}}_o(\bar{r},s) \cdot \bar{J}_i^I(\bar{r}) \, dS, \tag{10}$$

where $\tilde{\bar{\bar{E}}}_o(\bar{r},s)$ is the propagation factor portion of the excitation field, i.e. we factor the total excitation as

$$\tilde{\bar{\bar{E}}}(\bar{r},s) = \tilde{f}(s_i)\, \tilde{\bar{\bar{E}}}_o(\bar{r},s). \tag{11}$$

Finally, the constants β_i^o may be determined from (8) since all other factors in the expression are known. Viz.

$$\beta_i^o = \frac{A_{ij}^o}{\eta_i^{(1)o}\, \tilde{f}(s_i)\, \hat{p}_j \cdot \bar{J}_i^o(\bar{r}_j)}. \tag{12}$$

It should be pointed out that the index j appears in the right-hand side of (12). However, $\hat{p}_j \cdot \bar{J}_i^o(\bar{r}_j)$ is proportional to A_{ij} so the ratio in (12) is constant with respect to j.

In summary the key steps in the extraction are as follows:

1. Apply a Prony-type algorithm to spatially-sampled transient currents.
2. Construct an approximate natural mode from the spatial variation of the residues obtained for a single pole per (8) and (9).

3. With the coupling coefficient computation as an intermediate step, compute the normalization constants β_i.

The resulting data within the limitations of completeness outlined in the following section may be reexpanded to provide transient currents under new excitation conditions. This reexpansion can be carried out formally with Class 1 or Class 2 coupling coefficients since the modes and normalization constants are known explicitly.

2.2 Signal Processing Considerations

Most data analyzed by this process is likely to be plagued by noise whether obtained numerically or experimentally. Dudley [7] has shown when the least-square Prony procedure is applied to data containing noise, the resulting poles are biased in the estimate of the real part. Therefore, if a Prony-type technique is to be used as a practical tool it must be tolerant of noise in the data it analyzes.

We know that a given object possesses poles which are intrinsic to it alone. However, the pole sets computed from the many sampled current waveform observations along the structure are not identical. Therefore, a technique is used to form the best observed pole set for the structure which we term the "consensus pole set."

To form a consensus pole set we follow the steps below:

1. Use a pole extractor to obtain pole sets from each observed waveform;
2. Display these pole sets graphically, and group only the poles which tend to form a cluster, as illustrated in Figure 2;
3. Take the average value of the poles grouped;
4. These spatially averaged poles and only these averaged poles

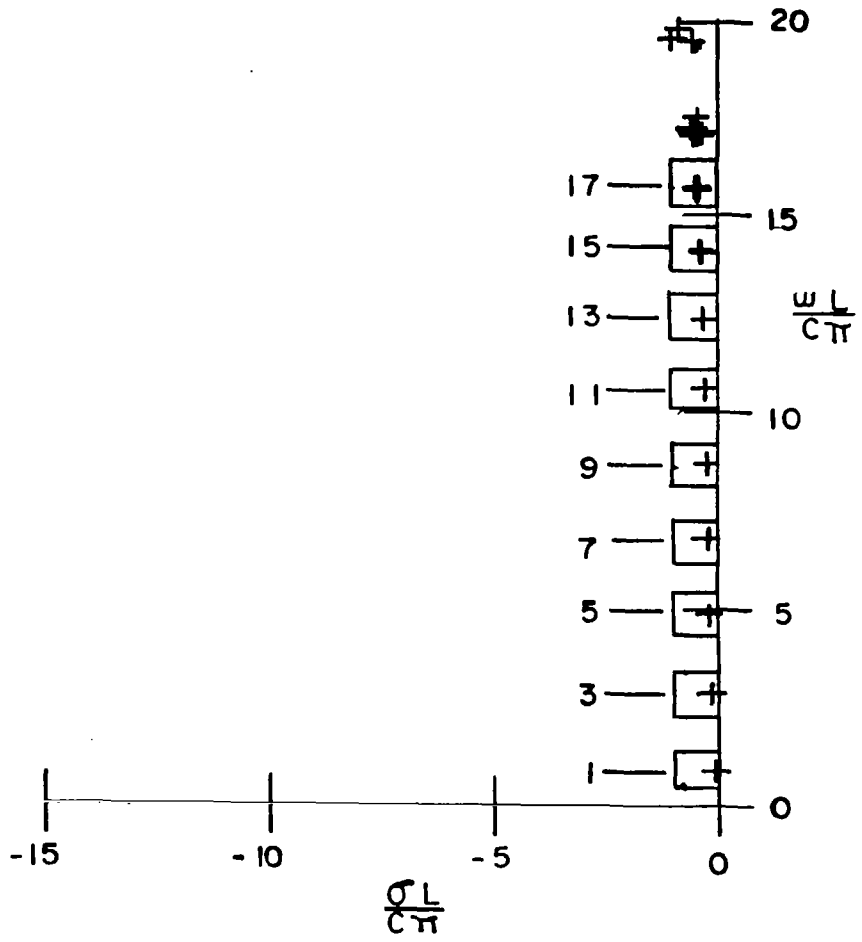

Figure 2. Groupings of poles which occur in obtaining the consensus pole set. For the lower-order poles a single + is shown, which is actually an overlay of 17 poles on top of each other.

constitute the consensus pole set. Any other poles present are presumed to be "curve fitting" poles [6] and are discarded; and

5. Use this consensus pole set alone to obtain corresponding residues for each sampled waveform and the remaining SEM description.

This procedure is essentially the "cluster averaging" method used by Lager, et al. (8) in their sliding-window Prony technique. It is applied here to exploit spatial rather than temporal redundancy in the data.

The pole extractors used in this work were the least-squares Prony procedure after Van Blaricum and Mittra [6], and the sliding-window Prony procedure after Lager, et al. [8]. Because of its computational efficiency, the least-square Prony procedure was used whenever the data exhibited a low level of noise. A set of poles was obtained for each waveform. These pole sets were associated as described above to yield the consensus pole set. However, when noise levels were encountered with magnitudes severe enough to make clusters unidentifiable, the sliding-window Prony procedure was used. This occurs, for example, in numerical data when the wire is locally-driven near its end where coupling is weak.

In summary, a set of poles for each sampled waveform is obtained by an appropriate pole extraction technique. The poles are graphed, those which aggregate in clusters are grouped and averaged. The averaged poles and only these poles constitute the consensus pole set. The residues are calculated for an expansion in terms of the consensus pole set alone.

2.3 Data Completeness Considerations

The general SEM description for a system consists of an infinite collection of data. However, when applied to measured or computationally derived results only a finite collection of data can be obtained. Therefore, the question of data completeness arises.

In general, one would likely want to acquire sufficient data to acquire spatially-complete data within a predefined bandwidth.

There are two mechanisms which limit the extent of the SEM data derivable from a given collection of transient data: the extent of the frequency spectrum of the time history of the excitation; and the coupling between the spatial form of the excitation and individual modes.

The band-limiting of the frequency spectrum limits the resonances which are excited. Hence, if one wishes to recover high-order poles, he must use an excitation which is sufficiently broadband to excite the resonances desired to an amplitude well above the noise level of the data.

The spatial placement and/or distribution of the excitation can be such that it has a small or zero coupling coefficient for certain modes. For example, Figure 3 illustrates a center-driven cylinder and the first antisymmetric mode on a cylindrical structure. The generator is located at a null of the mode. Thus, in the coupling coefficient integral of (10), this excitation/mode combination yields a zero coupling coefficient. Even if the generator were slightly off center, the coupling coefficient, though non-zero, would be small. The associated resonance would be only weakly excited. Hence it could be lost in noise.

The end in obtaining the SEM description is to be able to extrapolate to new excitations. However, if the description is incomplete, either in the spectral or the spatial sense, then extrapolation cannot be carried out for a general excitation. In the spectral sense, the extrapolation cannot be extended beyond the band limitation of the description. In the spatial sense, the SEM description cannot be expanded to situations which properly couple data not present. For example, if an even excita-

tion were used to produce the data on which the extraction process operates, then the SEM description will contain only even modes and can be extrapolated to even excitations.

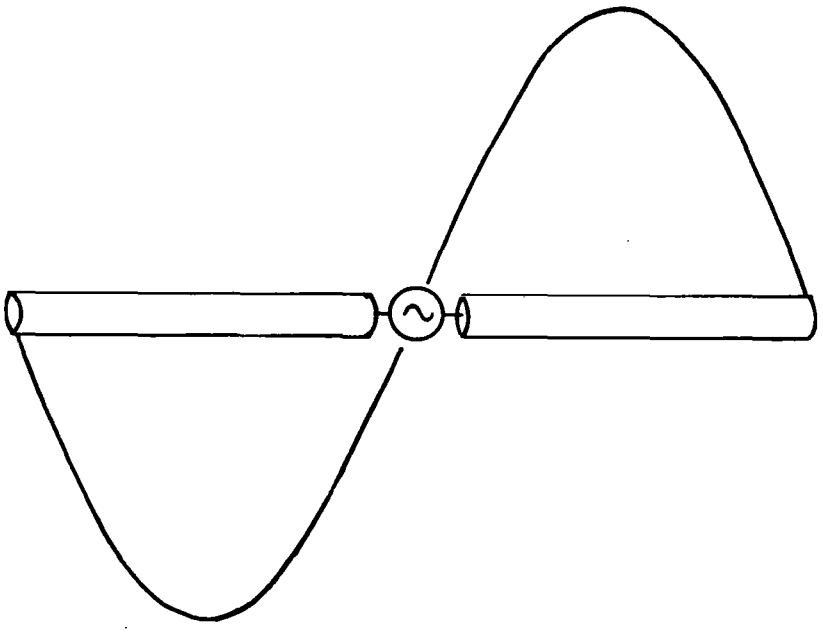

Figure 2. Mode 2 of a thin cylindrical scatterer which does not couple for the center excitation shown. The coupling coefficient for this case would be zero.

CHAPTER III

EXTRACTED SEM RESULTS

3.1 Introduction

This Chapter reports the SEM results extracted from several different collections of transient data using the method described in the preceding Chapter.

The transient data were obtained using the time domain computer code TWTD [13]. The structure modeled by TWTD was a thin cylindrical scatterer. This structure was chosen because of the availability of comparative SEM results obtained by Tesche [14] and because of the simplicity incumbent with the one-dimensional structure.

A 1-meter dipole antenna with a half-length to radius ratio of 100 was modeled by TWTD using 49 spatial segments. The excitation was defined to be a local generator occupying a single zone. Figure 4a illustrates the segmentation, and shows the numbering scheme used.

For excitation, a Gaussian waveform in time was chosen, having the form

$$v_g(t) = e^{-\left(\frac{t-T_m}{T_w/2}\right)^2}$$

where T_m is a time shift chosen to produce quasi-casuality, and Tw, termed the waist of the Gaussian, is used to adjust the spectrum of the excitation in the frequency domain. As evidenced by Figure 4b, the waist of the Gaussian is defined as the width of the Gaussian at 36.8 percent of its peak value, or the 1/e point.

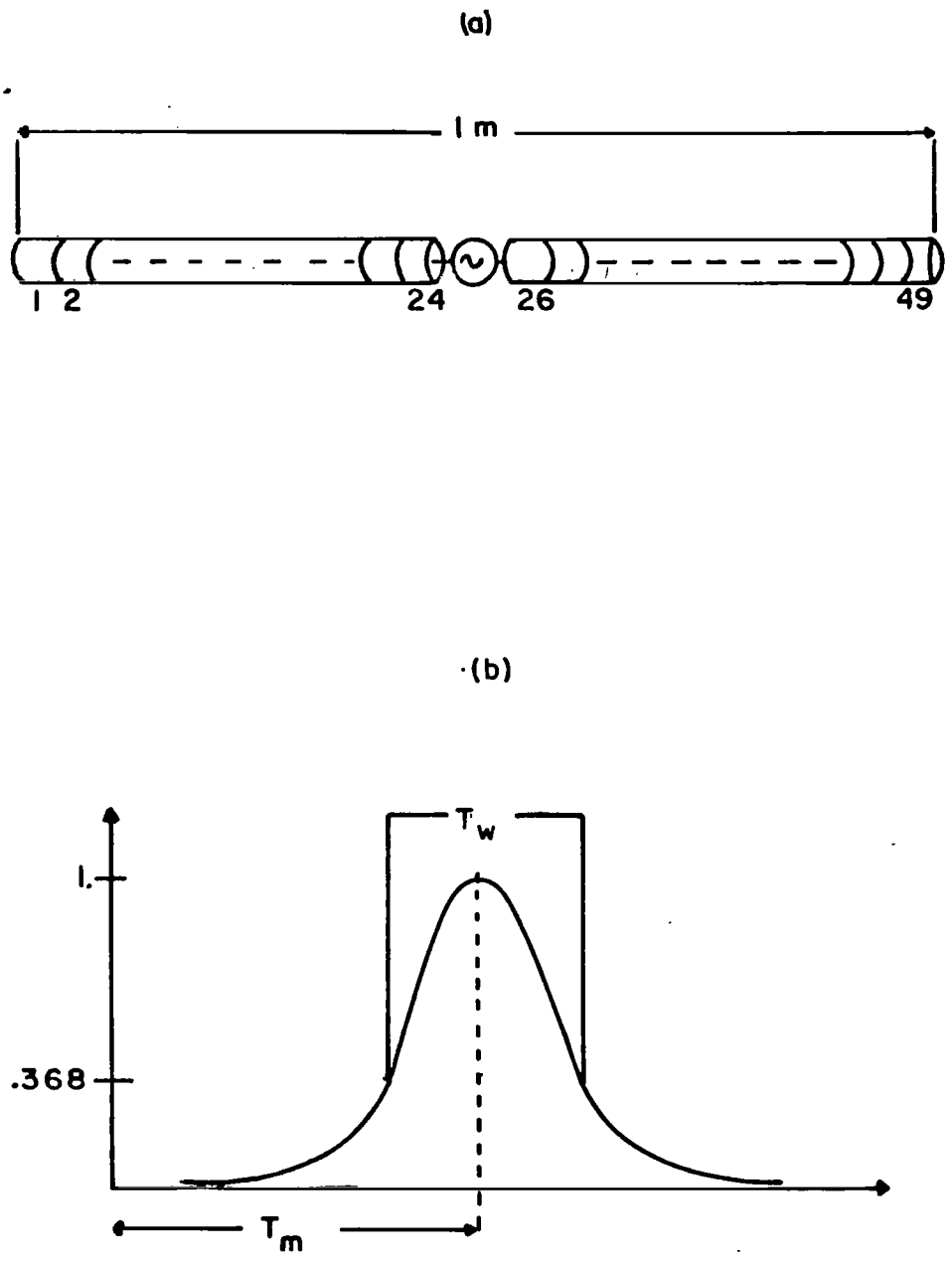

Figure 4. (a). TWTD model of the wire scatterer with the generator at the center segment: zone 25. The order of segmentation is also shown. (b). Model of the Gaussian generator used for excitation, showing the "waist" parameter.

3.2 The Influence of the Spectrum of the Excitation on Recoverable Poles

As we pointed out in the preceding Chapter, in order for a given resonance to be recoverable, the excitation function must possess a spectral component which excites the resonance appreciably. The examples which follow demonstrate this phenomenon clearly.

In the following two examples, we extract poles from TWTD data. Two different Gaussian pulse widths are used for the generator, and the generator is located at the center of the structure (zone 25) in each case.

For each excitation the least-squares Prony procedure was applied to 17 different observation waveforms, where 12 pole pairs were obtained and plotted. Only the poles corresponding to even natural mode functions are present, since the odd poles are not excited for a center excitation.

In Figures 5 and 6 the spectrum of the Gaussian excitation, and the spatial pole clusters obtained for each example are shown. The poles within a spatial cluster are grouped and averaged to form an element of the consensus pole set. The data shown in Figure 5, Example 1, are for a Gaussian excitation whose waist is 0.6158 nanosecond. By examining the spectrum shown for this excitation, we notice at the 7th resonance the value of the forcing function's spectrum is nearly zero. Therefore we would not expect our forcing function to excite poles at higher frequencies. Comparing our conclusion with the actual poles extracted shows pole number 7 to be the highest pole cluster which is explicitely identifiable. The "curve fitting poles" which Van Blaricum and Mittra [6] describe appear near possible higher frequency clusters and render their identity doubtful.

The data in Figure 6, Example 2, are those generated by a Gaussian forcing function whose waist is 0.3077 nanosecond. Here, pole clusters

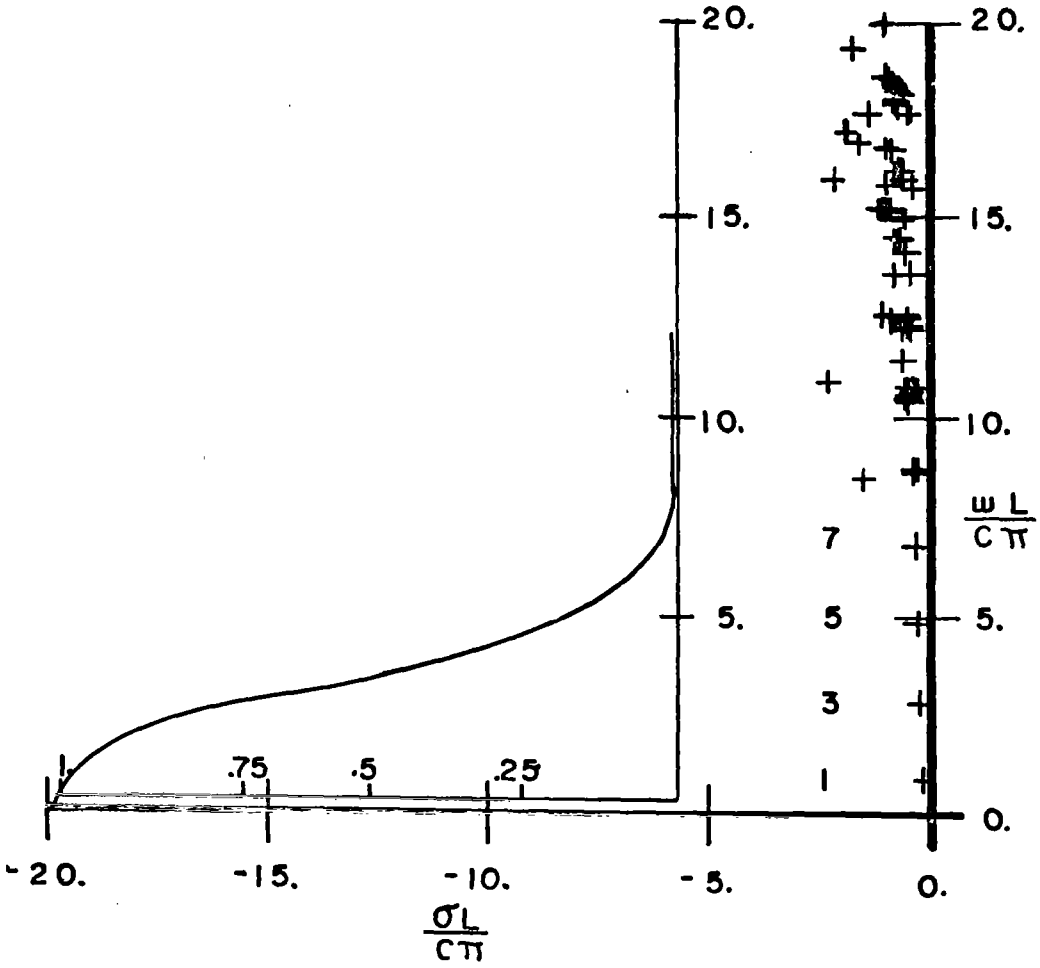

Figure 5. The spectrum of the Gaussian forcing function, with a waist of 0.6158 nanoseconds, shown with the poles extracted from the transient response it generated: Example 1. Note the scattering of the poles above pole 7.

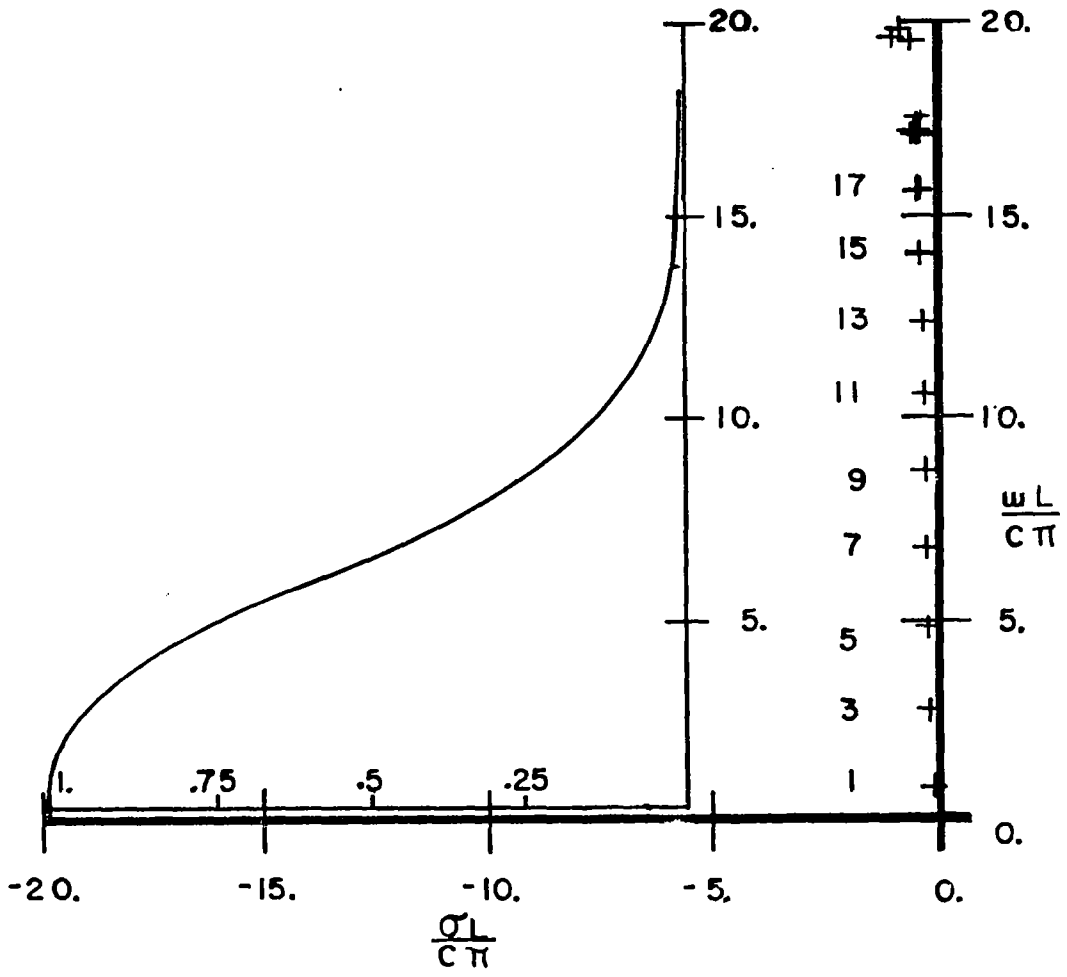

Figure 6. The spectrum of the Gaussian forcing function, with a waist of 0.3077 nanoseconds, shown with the poles extracted from the transient response it generated: Example 2. Note the scattering of the poles above pole number 17.

are identifiable through pole 17. This is commensurate with the spectrum of the excitation.

3.3 Extracted SEM Parameters - Even Mode Case

The extraction technique described in Chapter II has been applied for the cases described in the previous section. The identifiable poles were grouped and averaged to form consensus pole sets. Residues were extracted according to the least-square Prony procedure using the consensus pole set; i.e. the "curve fitting poles" were discarded and cluster average values used. The data which follow compared with those given by Tesche [14]. Tesche's data comprise only modes 1 through 12. Thus no comparisons are possible for modes 13 through 17 in the second case studied.

The consensus poles and the poles reported by Tesche are compared in Table 1. The nine poles determined in Example 1 agree well with Tesche's. Notice that we included the ninth cluster even though there is some question as to whether this cluster is "identifiable." Subsequent results, however, evidence poor quality in the mode corresponding to this pole.

The poles from Example 2 compare well to those reported by Tesche, and exhibit a consistent trend for the poles beyond. However, no comparison is available for these higher frequency poles so the exact accuracy is not known.

Figures 7 through 12 are comparisons of the extracted modes with those of Tesche. Every mode obtained for Example 2 is given, while only selected modes are given for Example 1.

Figure 7 displays mode 1 and 7, corresponding to poles number 1 & 7 respectively for Example 1. All of the odd-numbered modes of Example 1 are essentially indistinguishable from those of Tesche. Figure 8

TABLE 1

Consensus Poles and Those Reported by Tesche

Pole Index	POLE VALUES					
	Tesche sL/c		Example 1 sL/c		Example 2 sL/c	
	Real	Imag	Real	Imag	Real	Imag
1	-0.082	0.926	-0.082	-0.918	-0.082	0.918
3	-0.147	2.874	-0.148	2.878	-0.148	2.878
5	-0.188	4.835	-0.189	4.844	-0.189	4.844
7	-0.220	6.800	-0.222	6.789	-0.221	6.796
9	-0.247	8.767	-0.256	8.710	-0.248	8.717
11	-0.270	10.733			-0.278	10.600
13					-0.317	12.392
15					-0.372	14.101
17					-0.435	15.714

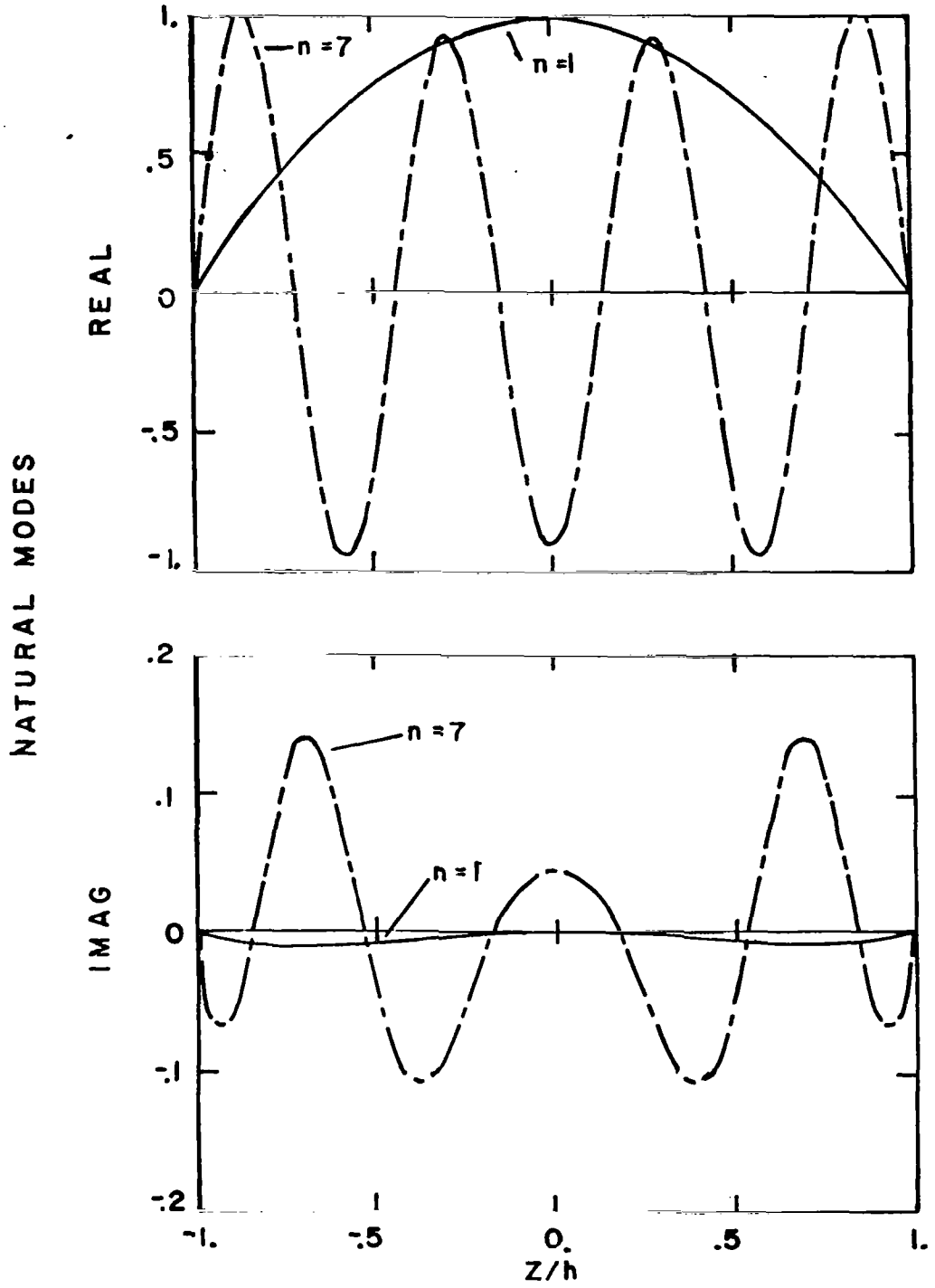

Figure 7. Real and imaginary parts of modes 1 and 7 obtained from the transient data of Example 1. Tesche's modes are indistinguishable from these.

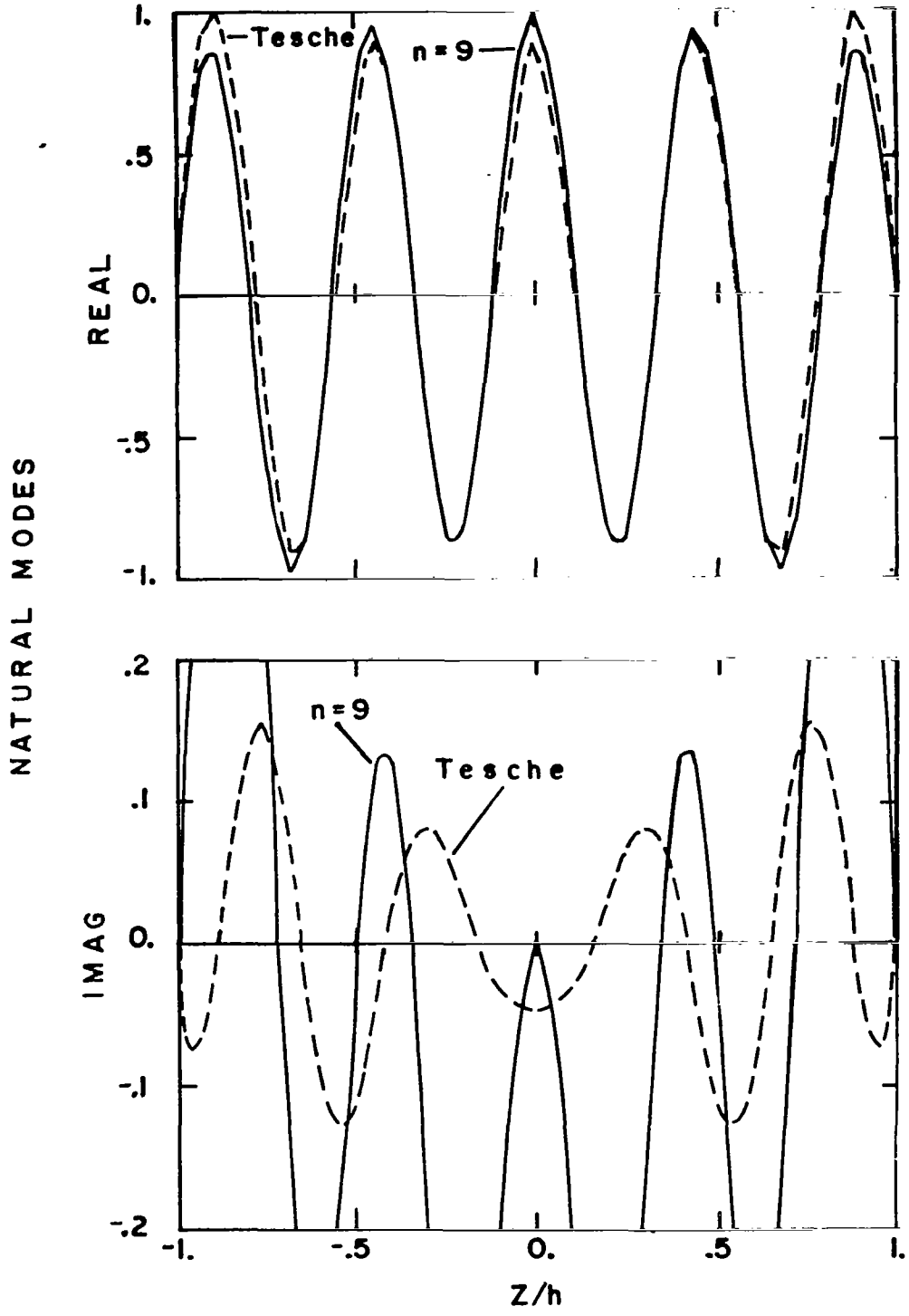

Figure 8. Real and imaginary parts of mode 9 obtained from the transient data of Example 1 compared with that of Tesche.

compares the extracted mode 9 with Tesche's corresponding mode. The comparison is seen to be unsatisfactory, particularly in the imaginary part. The excitation spectrum is too small at this pole to provide a recoverable mode. Recall that the spectrum significantly excited only through the seventh mode and it is questionable as whether the 9th pole should have been included in the consensus pole set in the first place.

The modes of Example 2 are shown in Figures 9 through 12. Modes 1 through 11 agree favorably with Tesche's, but since he reported only these eleven modes, comparison of higher modes is not possible. However, the higher modes show the features one would expect.

Table 2 gives a comparison of Tesche's normalization constants with those of both the preceding Examples. We see from the Table that the normalization constants from Example 1 compare well with Tesche's through pole 7. The results of Example 2 agree with Tesche's results favorably for all the poles reported. The departure between the two, though satisfactory, cannot be overlooked in constants 9 and 11. The constants seem to grow too rapidly for poles 13 and beyond. The precise cause for this phenomenon has not been investigated.

3.4 Extracted SEM Parameters - General Case

For Example 3 the forcing function is placed at a position of 0.367 L from the end of the wire: segment 18. Example 4 has the forcing function applied at 0.2499 L from the end: segment 12. The waist of the Gaussian forcing function in these examples is 0.3077 nanoseconds.

Table 3 contains Tesche's poles and the consensus pole sets from Examples 3 and 4. The sliding-window Prony procedure was used to obtain these data using five subsequences per waveform. (For these examples the

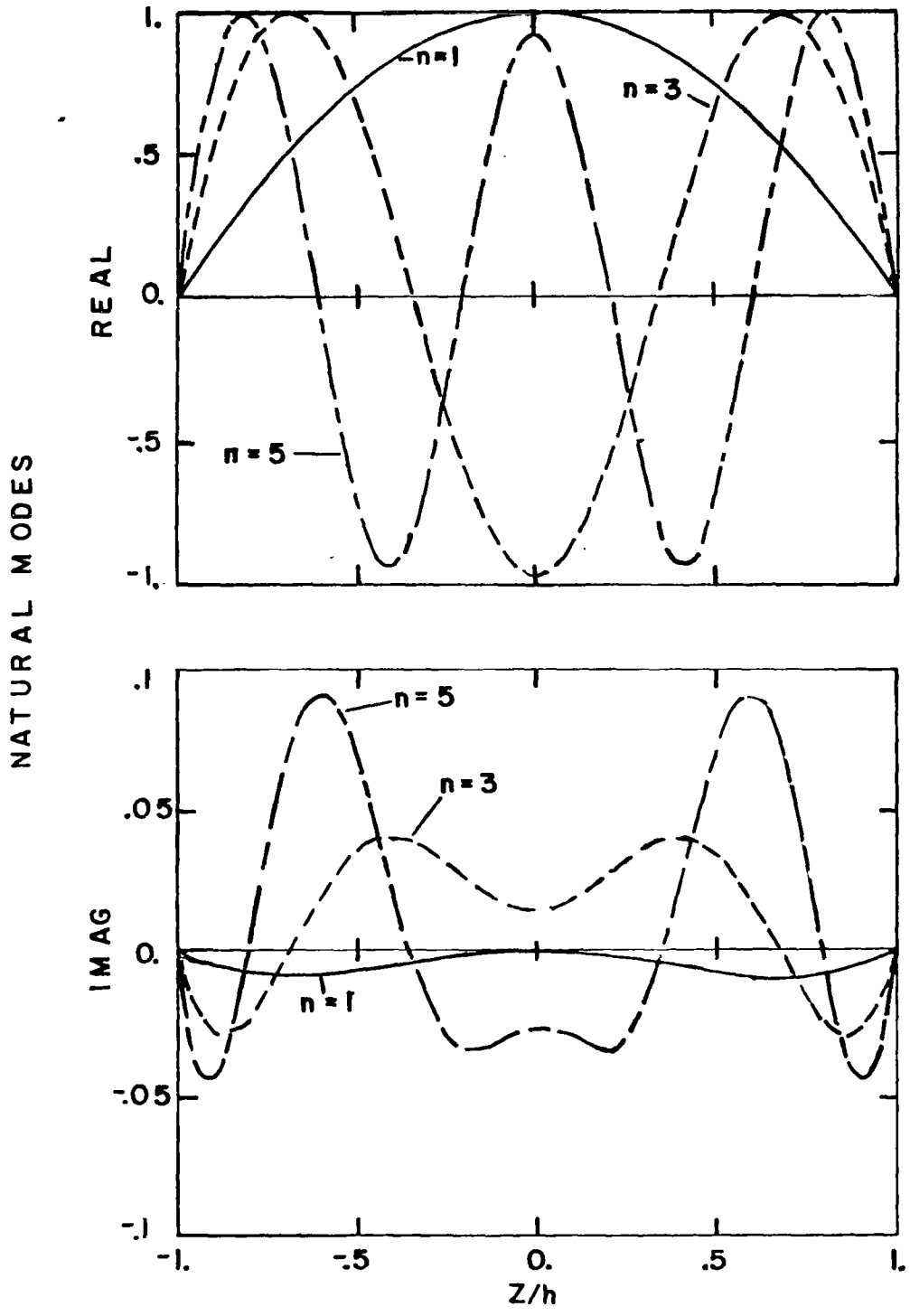

Figure 9. Real and imaginary parts of modes 1, 3, and 5 derived from the transient data of Example 2. Tesche's corresponding modes are indistinguishable from these.

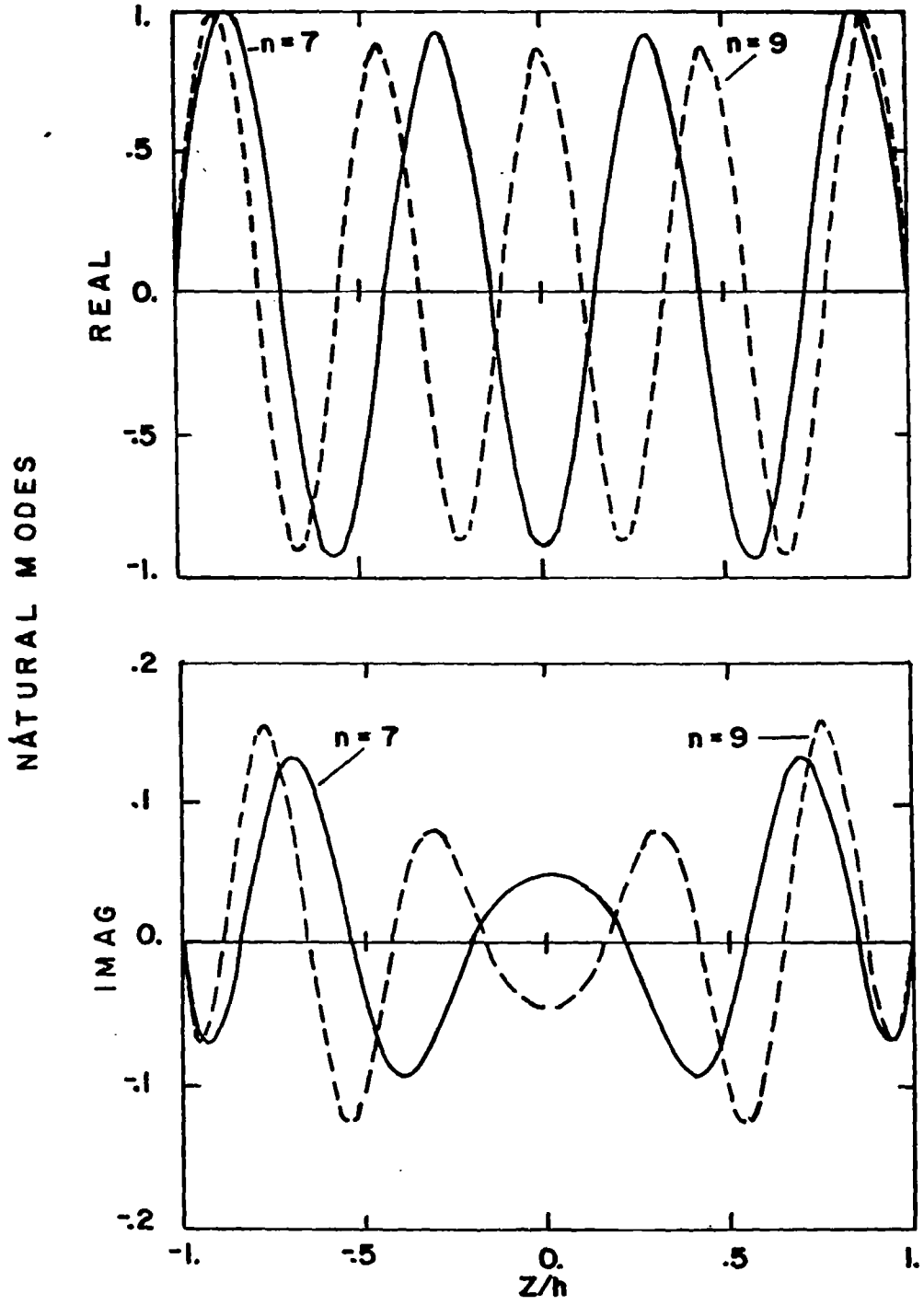

Figure 10. Real and imaginary parts of modes 7 and 9 derived from the transient data of Example 2. Tesche's corresponding modes are indistinguishable from these.

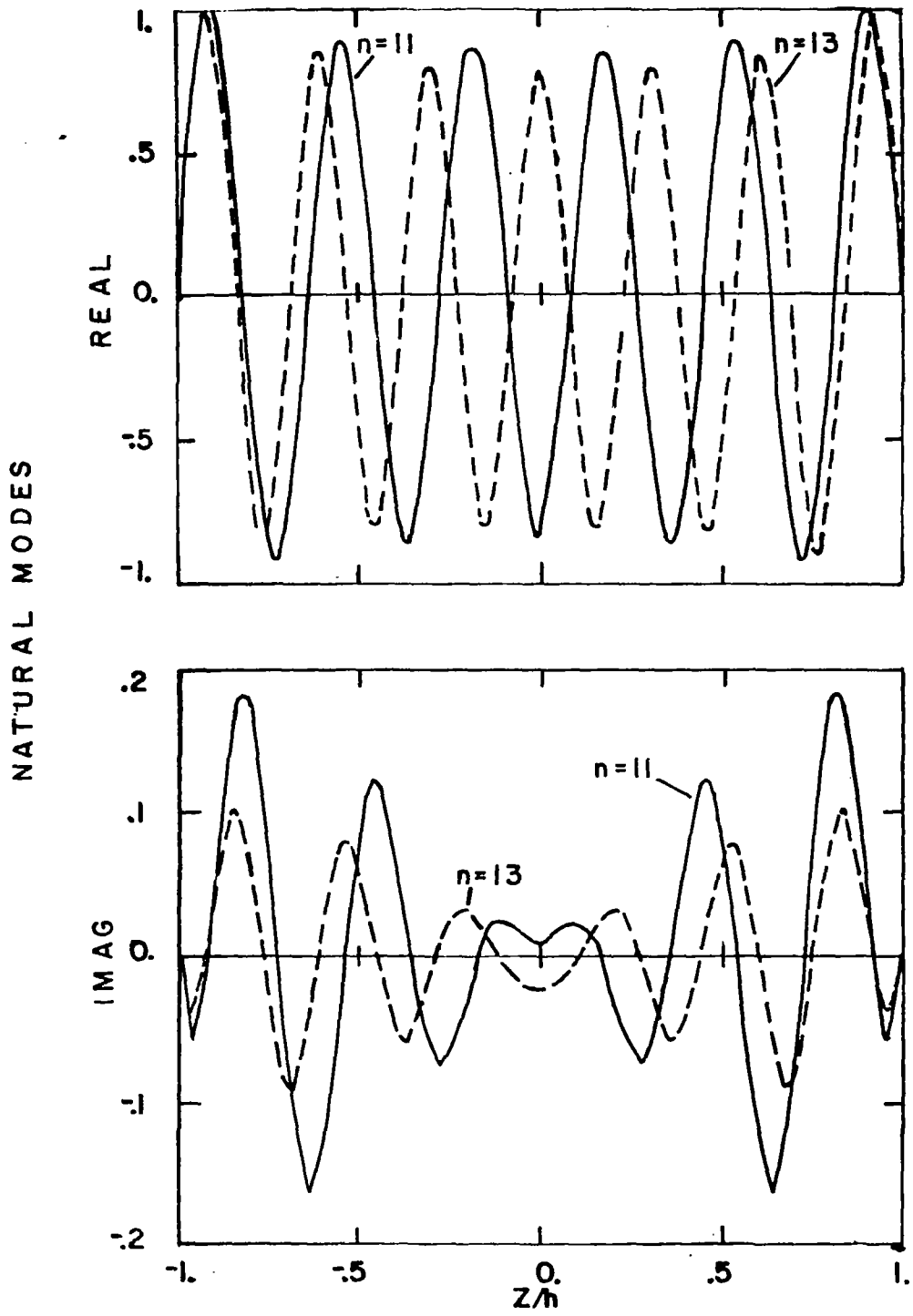

Figure 11. Real and imaginary parts of modes 11 and 13 derived from the transient data of Example 2. No comparisons are available, however the oscillation one would expect is present.

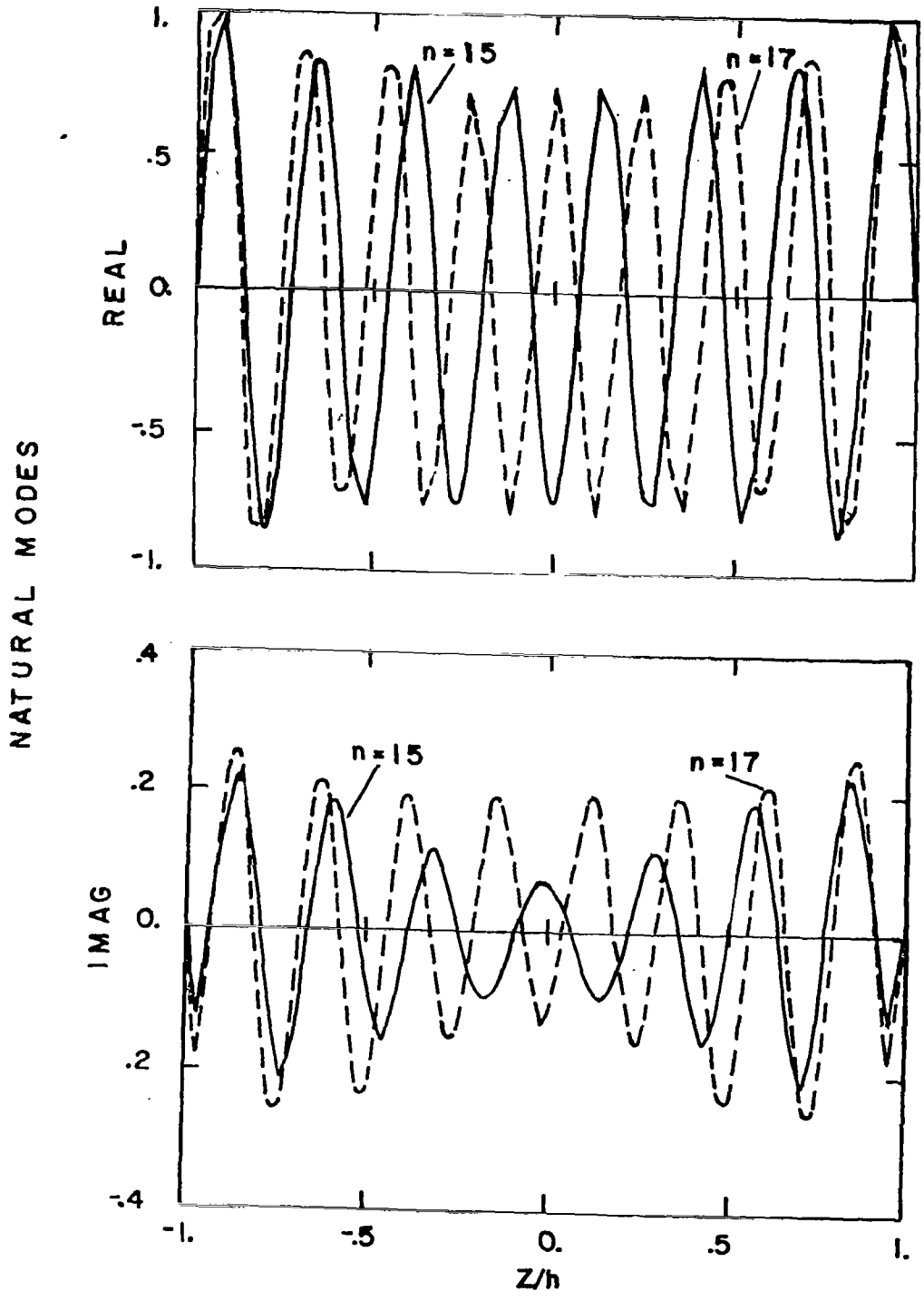

Figure 12. Real and imaginary parts of modes 15 and 17 derived from the transient data of Example 2. No comparisons are available, however the oscillation one would expect is present.

TABLE 2

Transient Extracted Normalization Constants and Those Reported by Tesche

Pole Index	NORMALIZATION CONSTANTS					
	Tesche L/c		Example 1 L/c		Example 2 L/c	
	Mag	Angle	Mag	Angle	Mag	Angle
1	3.72	15.59	3.68	12.33	3.68	12.33
3	4.62	16.45	4.75	5.24	4.75	5.15
5	5.32	15.86	5.53	0.94	5.62	0.83
7	5.98	17.25	6.18	2.77	6.19	5.45
9	6.64	18.83	5.03	32.66	7.27	14.13
11	7.17	21.74			7.87	27.20
13					9.84	30.85
15					11.54	30.11
17					13.18	23.22

least-squares Prony procedure was first applied, but consensus clusters could not be identified.) Example 3 contains poles 1, 2, 4, 5, 7, 9, and 10, since the other poles are not coupled spatially for this excitation. In Example 4, poles 1, 2, 3, 5, 6, 7, 9, and 10 are coupled. Comparing pole values of Examples 3 with Tesche's poles we find good agreement for every pole. However, some small differences are noted in the comparisons of Example 4.

The natural modes for pole numbers 1, 2, and 5 are given in Figures 13 through 15, for each of these Examples. Extracted modes beyond mode 4 represent the poorest quality results obtained in this study. The essential oscillatory features still appear in the modes, but the zero crossings are shifted to a small degree and errors in peak amplitudes on the order of twenty percent are present. Precise modal symmetry or antisymmetry is generally lost by way of these two types of errors. Observing mode 1 of both Examples shown in Figure 13, we see that the mode of Example 3 is more nearly correct than that of Example 4. We conjecture this is due to the location of the generator for Example 3; i.e., mode 1 of Example 3 is more strongly coupled than mode 1 of Example 4 and hence better data is derivable. Figure 14 displays mode 2 for both Examples. For this mode, the Example 4 result is more strongly coupled. Evidence of this is seen in the more stable imaginary part and proper zero crossings. Figure 15 shows mode 5 for both Examples. Here we see results for both Examples which are not particularly gratifying. Example 4 is seen to possess more nearly uniform amplitude peaks. We again conjecture this is due to the slightly stronger coupling of this mode in Example 4. Reexpanded results in the next Chapter show, however, that these errors do not strongly effect extrapolated results so long as the spectrum for the reexpansion excita-

TABLE 3

Consensus Poles and Those Reported by Tesche

Pole Index	POLE VALUE					
	Tesche sL/c		Example 3 sL/c		Example 4 sL/c	
	Real	Imag	Real	Imag	Real	Imag
1	-0.082	0.926	-0.078	0.934	-0.092	0.922
2	-0.120	1.897	-0.124	1.862	-0.159	1.916
3	-0.147	2.874	*		-0.139	2.789
4	-0.169	3.854	-0.168	3.918	*	
5	-0.188	4.835	-0.189	4.845	-0.168	4.807
6	-0.205	5.817	*		-0.259	5.853
7	-0.220	6.800	-0.230	6.812	-0.221	6.797
9	-0.247	8.767	-0.248	8.718	-0.265	8.926
10	-0.260	9.752	-0.272	9.598	-0.284	9.668

*Resonance not observable for this excitation.

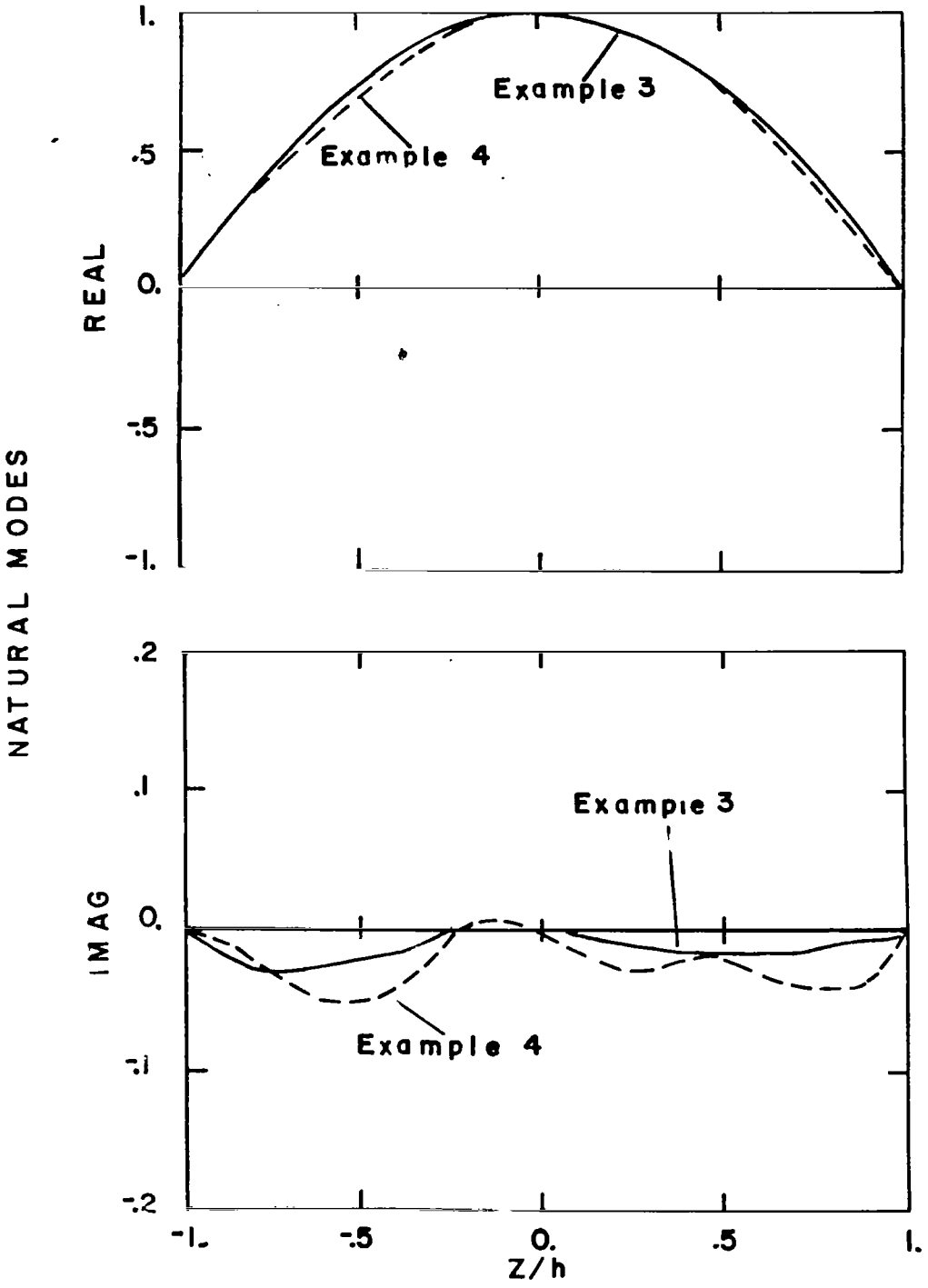

Figure 13. Real and imaginary parts of mode 1 derived from the transient data of Examples 3 and 4: off center excitation.

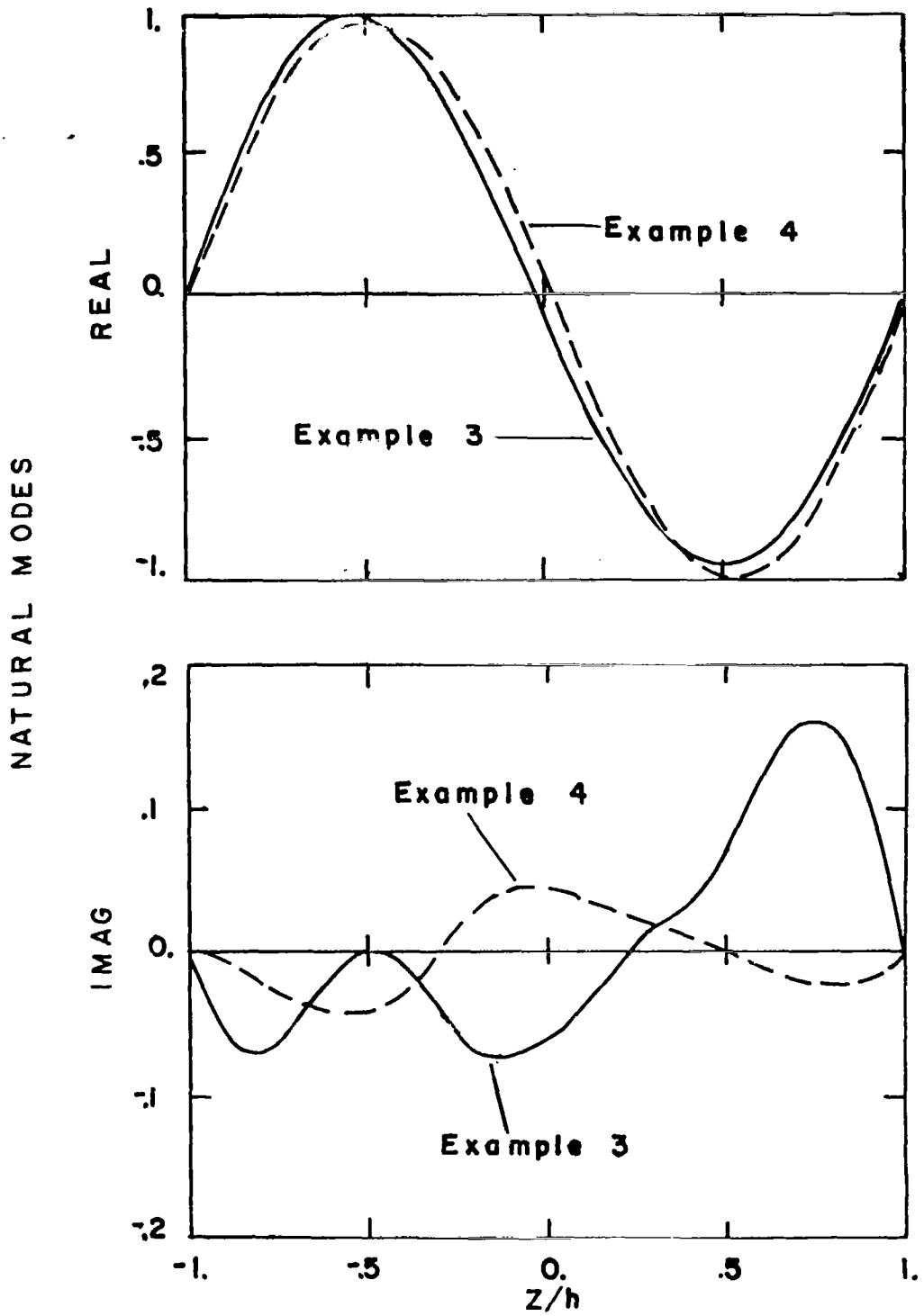

Figure 14. Real and imaginary parts of mode 2 derived from the transient data of Examples 3 and 4: off center excitation.

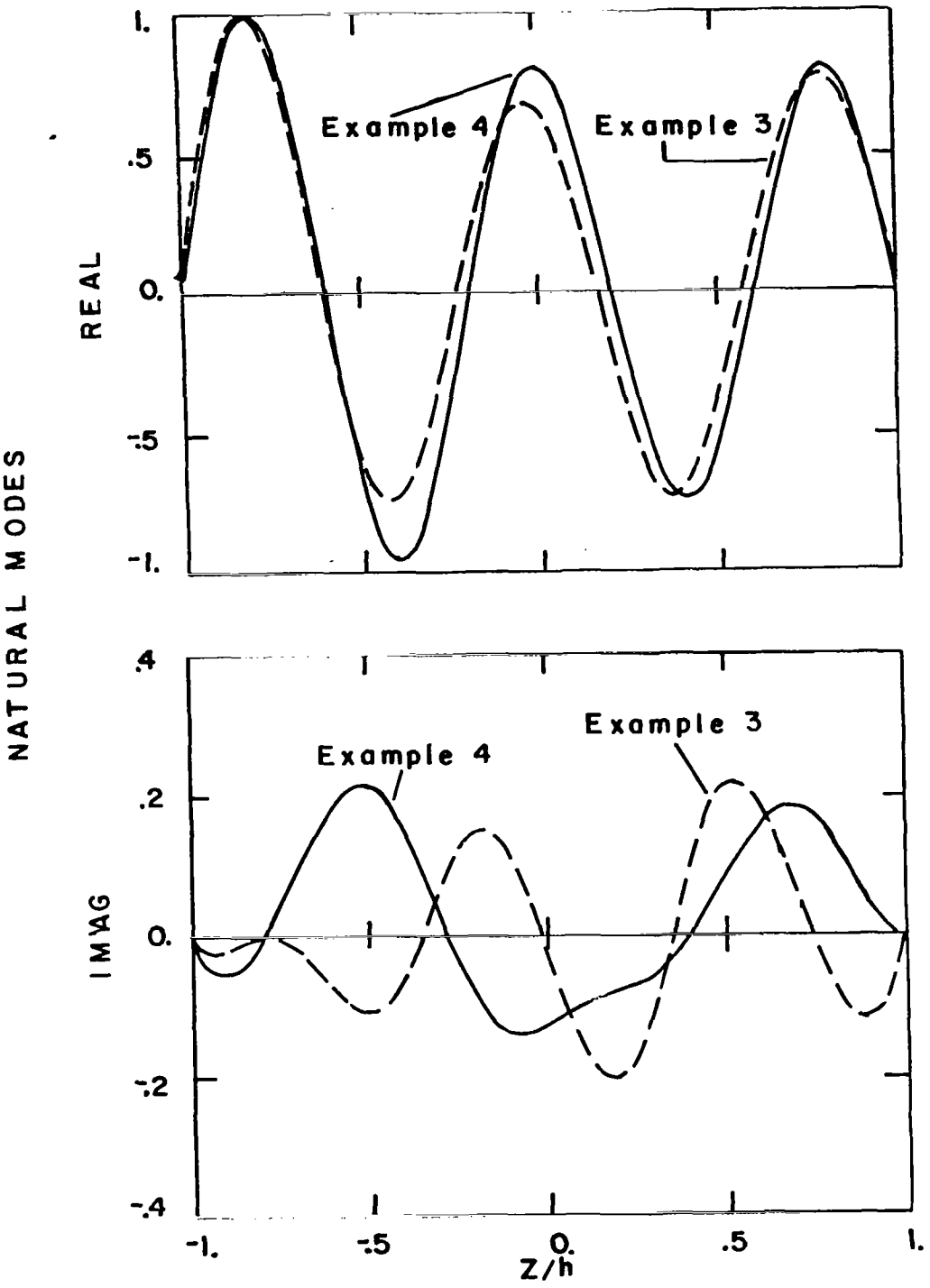

Figure 15. Real and imaginary parts of mode 5 derived from the transient data of Examples 3 and 4.

tion does not differ drastically from that of the source data.

Table 4 contains the magnitudes and phases of Tesche's normalization constants and those of both Examples. Comparing the constants of these examples to Tesche's we find relatively good agreement for constants associated with pole number 1. Comparing the constants of pole number 2, we see the value for Example 3 is much closer to Tesche's value than Example 4. These errors may be traced to the larger pole errors present in the Example 4 result. For example, the real part pole value for the second pole is in error by approximately 32.5 percent, resulting in a normalization constant whose magnitude is in error by 38.9 percent.

The errors in the normalization constants beyond the fifth one are quite large - several hundred percent at times. This is due largely to the fact that they are derived from a localized excitation and that the local errors in the modes are often large in these examples. The use of several generator locations in a given extraction procedure and disturbed excitation is expected to control this source of error.

The results associated with pole 5 in Example 3 demonstrate another mechanism for the intrusion of error. The extracted pole value itself is satisfactory. However, the generator location is such that the mode contributed only weakly in the total response. Observation of Figure 15 shows how the mode for this pole is corrupted because of the nearness of its contribution to the noise level. This error in the mode, in turn, propagates into the evaluation of the normalization constant.

TABLE 4

Transient Extracted Normalization Constants and Those Reported by Tesche

Pole Index	NORMALIZATION CONSTANTS					
	Tesche L/c		Example 3 L/c		Example 4 L/c	
	Mag	Angle	Mag	Angle	Mag	Angle
1	3.72	15.59	3.73	5.72	3.94	13.57
2	4.21	15.35	4.84	29.64	5.85	2.87
5	5.32	15.85	12.67	19.84	5.31	25.36

CHAPTER IV

EXTRAPOLATED RESULTS

4.1 Introduction

The utility of extracted SEM results lies in the ability to apply it to circumstances other than those through which the data were derived. This Chapter presents results obtained when the data described in the previous Chapter were used to characterize the thin-wire scatterer's response to several plane wave excitations.

For this extrapolation study, we created a complete SEM data base from transient extracted parameters. The data base was constructed from transient data excited by a Gaussian generator with a waist of 0.3077 nanosecond. The quantities associated with poles 1, 3, 5, 7, and 9 were derived from data excited by a generator located at the center of the wire, those associated with poles 2, 4, and 10 from data excited by a generator at 0.367 L, and those associated with pole 6 from the data excited by a generator at 0.245 L. Note that this data base does not include pole 8. The cases presented here do not require it in their representation. It may be derived readily from appropriate transient data. It was omitted for convenience here.

4.2 Gaussian Plane Wave Excitation

The transient extracted SEM data base was reexpanded using a plane wave with a Gaussian time history as the form of excitation, for 0, 30, and 60 degrees incidence, and the current was observed for each of these

angles at observation segments 0.245 the distance, 0.367 the distance, and half the distance from the end of the antenna. Two comparisons were used to check the validity of the transient extracted SEM reexpansion. The first is computed data for a direct time domain solution to the integral equation for the wire using the TWTD program. The second is a reexpansion in terms of SEM parameters obtained by a method of moments computation similar to that of Tesche.

Figure 16 displays transient currents computed by each of these means at 0 degrees incidence for the three observation points. Here we observe almost perfect agreement among the three, except in the early time. The reason for the disagreement in the early time is that only the pole contributions due to poles of the scatterer are included in the SEM expansions. The Gaussian excitation requires the inclusion of an entire function contribution in the inversion process. These data were generated primarily to observe the late time behavior of the extrapolated results. Consequently, this contribution was not included. A subsequent example for a different generator waveform allows early-time comparisons as well.

Figure 17 compares the currents from the three computations for 30 degrees incidence at the three observation points. In this Figure we again see good agreement in the late time. This comparison also manifests departures of the SEM expansion from the TWTD computation in the early time.

The currents excited by a plane wave incidence of 60 degrees are shown in Figure 18. The reexpansion for the transient parameters exhibit the essential features.

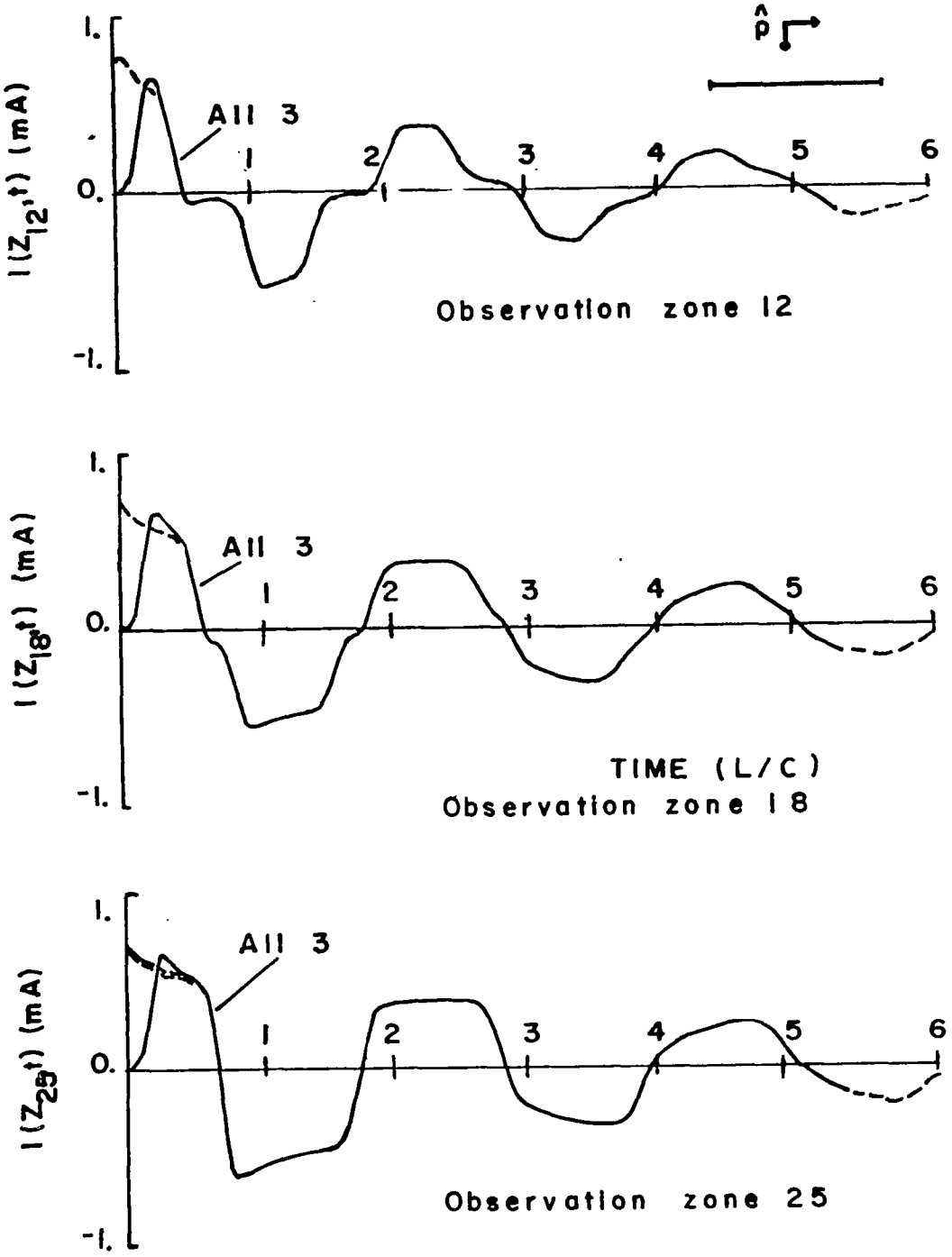

Figure 16. Transient currents for a plane wave with a Gaussian time history at 0 degrees incidence. Solid lines are from TWTD, dashed lines are from the expansion of SEM parameters obtained from an integral equation technique, and the dot-dashed lines are an expansion of the SEM parameters derived from transient data.

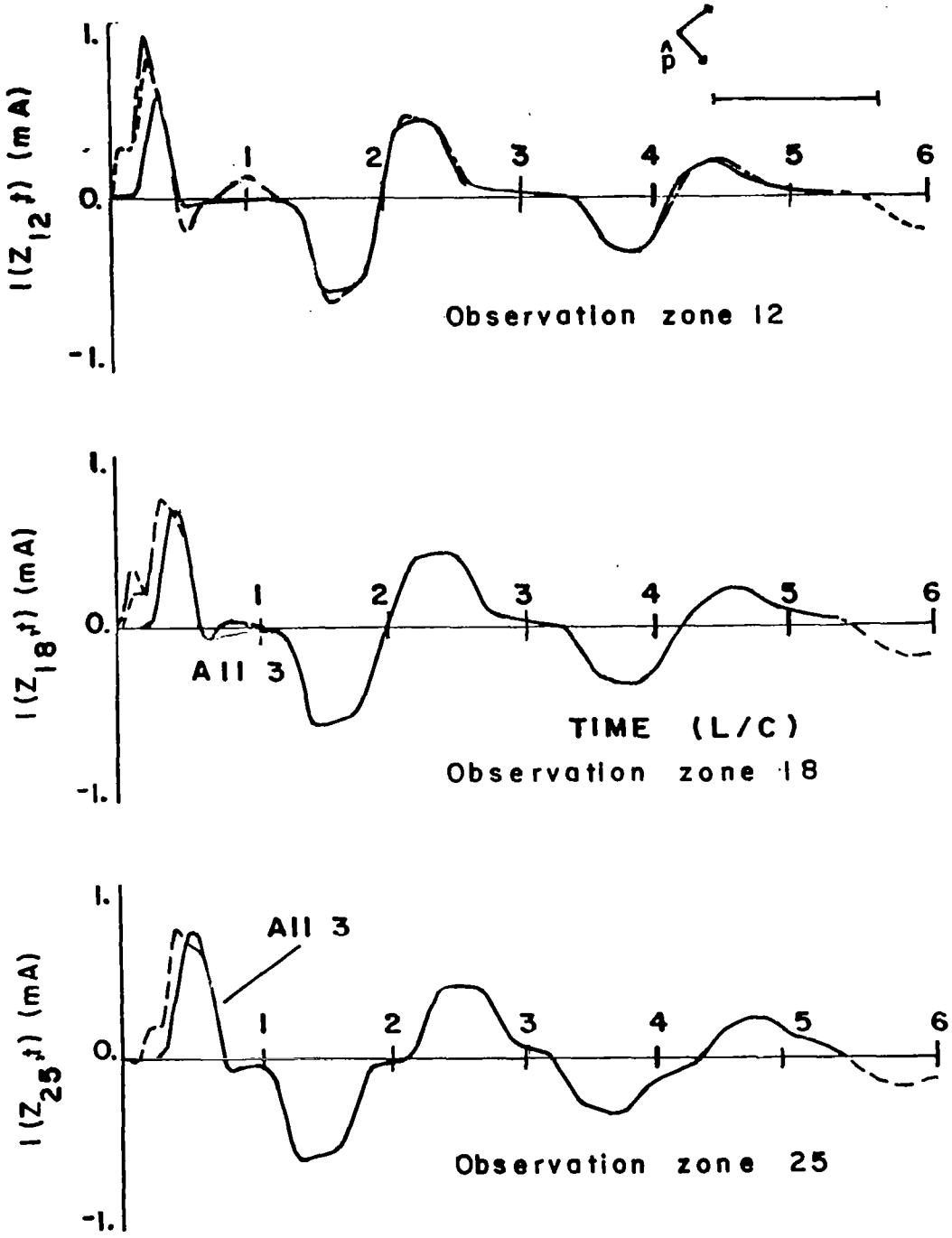

Figure 17. Transient currents for a plane wave with a Gaussian time history at 30 degrees incidence. Solid lines are from TWTD, dashed lines are from the expansion of SEM parameters obtained from an integral equation technique, and the dot-dashed lines are an expansion of the SEM parameters derived from transient data.

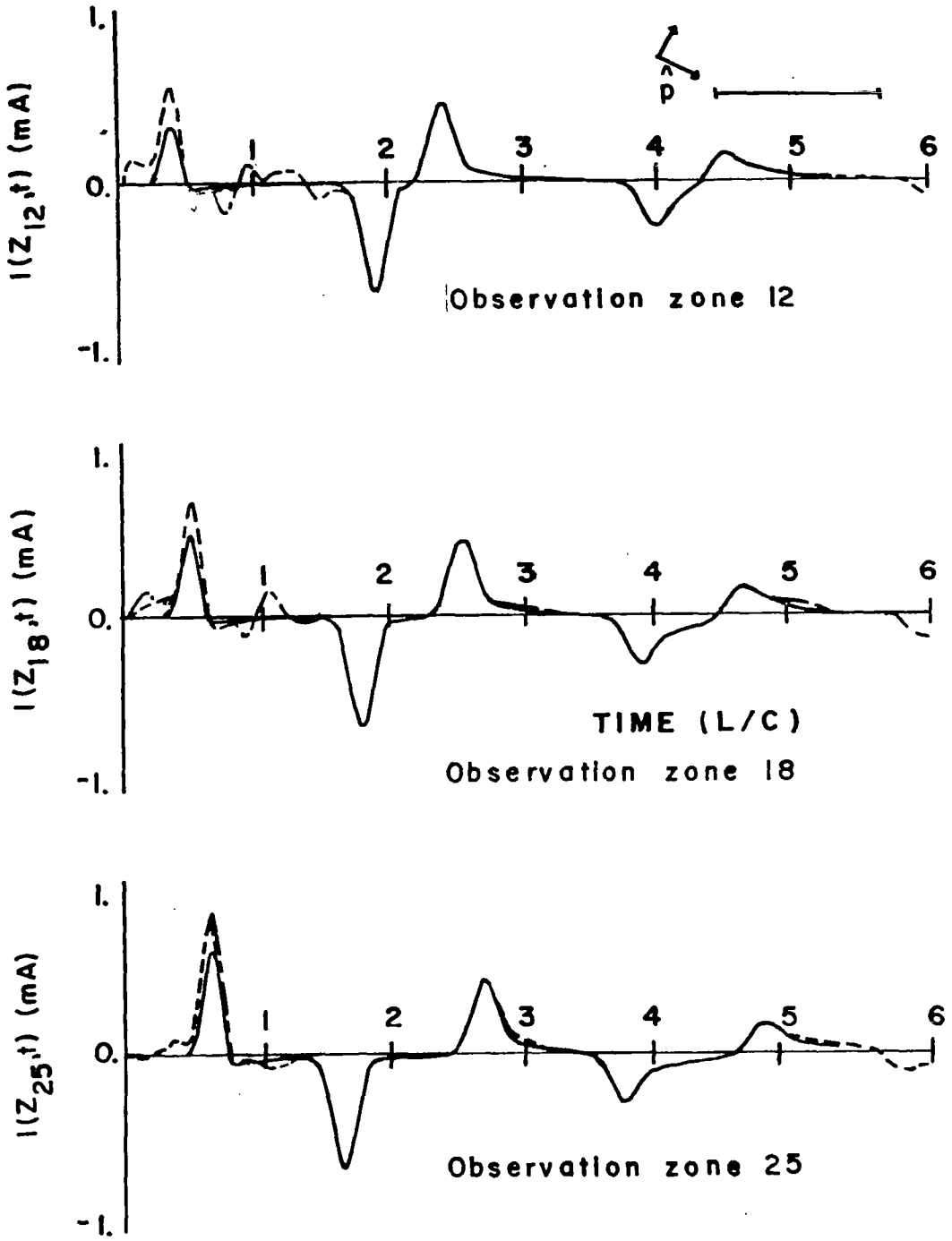

Figure 18. Transient currents for a plane wave with a Gaussian time history at 60 degrees incidence. Solid lines are from TWTD, dashed lines are from the expansion of SEM parameters obtained from an integral equation technique, and the dot-dashed lines are an expansion of the SEM parameters derived from transient data.

4.3 Reexpansion for Double Exponential Excitation

Using a plane wave with a double exponential time history as the excitation, the derived SEM data base was reexpanded for 0, 30, and 60 degrees incidence. The waveform pole contributions are included in these expansions. Thus we may compare early time results as well as the late time. The current was observed at observation zones 12, 18, and 25 for each excitation. These results were compared with a reexpansion in terms of SEM parameters obtained by a method of moments computation.

The transient current observed at the three observation segments at 0 degrees incidence is shown in Figure 19. We can see from this Figure the transient extracted reexpansion and the reexpansion for the method of moments data compare very well, in both the early and the late time.

Figure 20 displays the transient current at 30 degrees for the three observations. Here we see good agreement in the late time for observation zones 18 and 25, but some minor departure at zone 12 for both the early and late times. These departures can be attributed to the imperfect extracted modes and normalization constants.

The three observation zones for 60 degrees are shown in Figure 21. Here we see good agreement among the two cases for late time with some departure among the two in the early time.

In summary the reexpansion of the transient extracted data, in general, compares very well with the transient currents computed by TWTD, and the expanded SEM data derived by the method of moments. We therefore conclude that extrapolation of transient response data to new excitations using the Prony-based SEM extraction procedure is feasible.

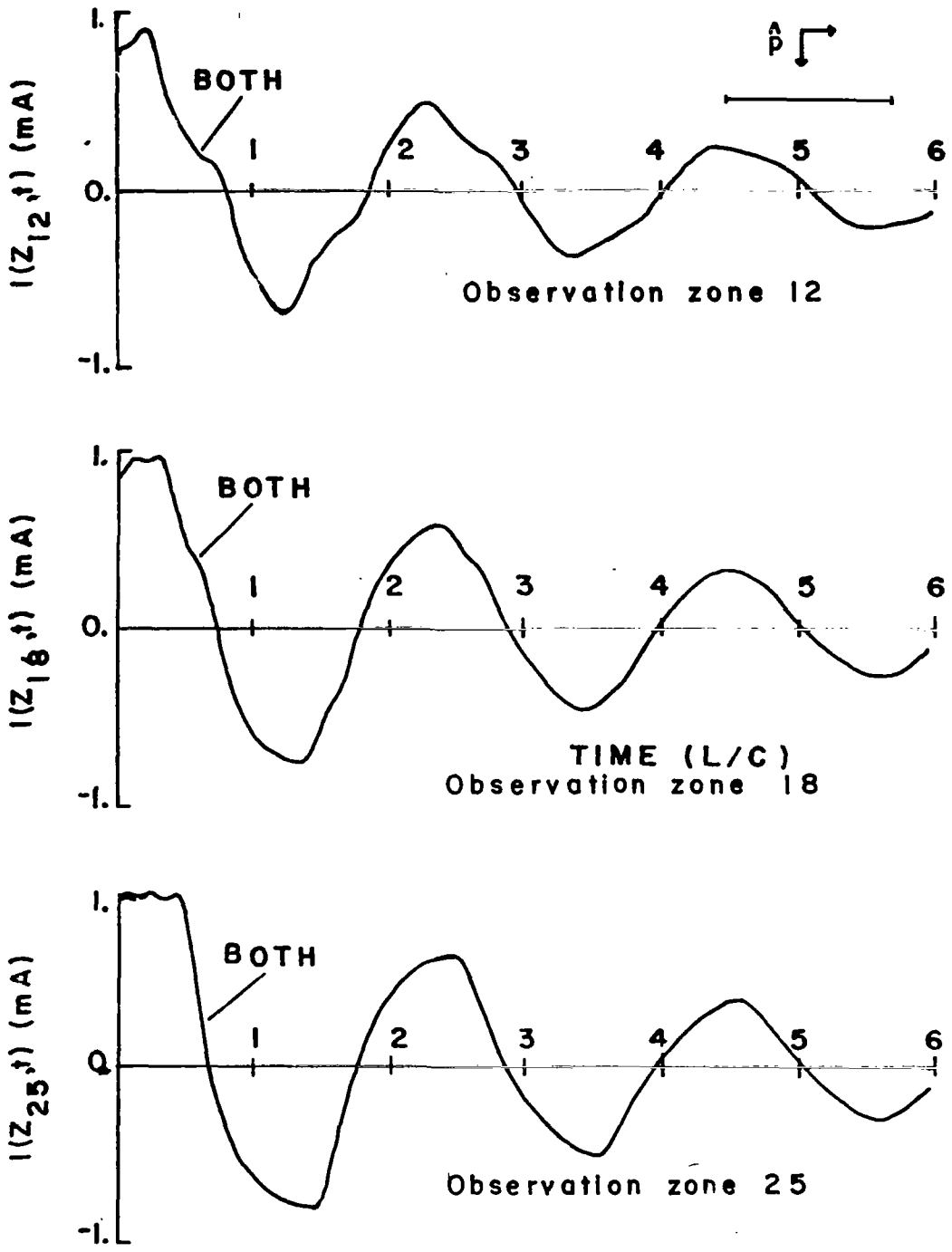

Figure 19. Transient currents for a plane wave with a double exponential time history at 0 degrees incidence. Solid lines are from an expansion of the SEM parameters derived from transient data, and the dashed lines are from an expansion of the SEM parameters obtained from an integral equation technique.

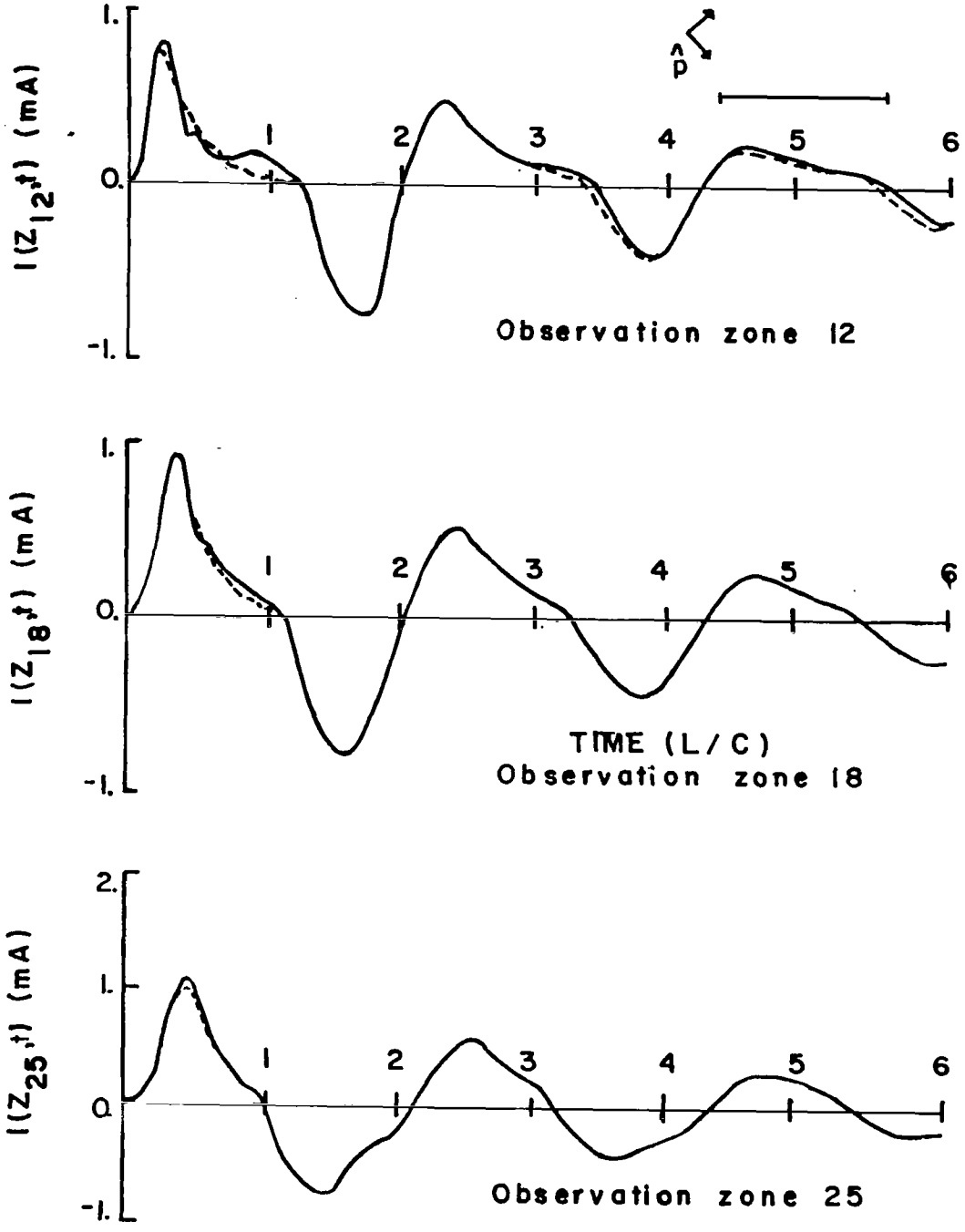

Figure 20. Transient currents for a plane wave with a double exponential time history at 30 degrees incidence. Solid lines are from an expansion of the SEM parameters derived from transient data, and the dashed lines are from an expansion of the SEM parameters obtained from an integral equation technique.

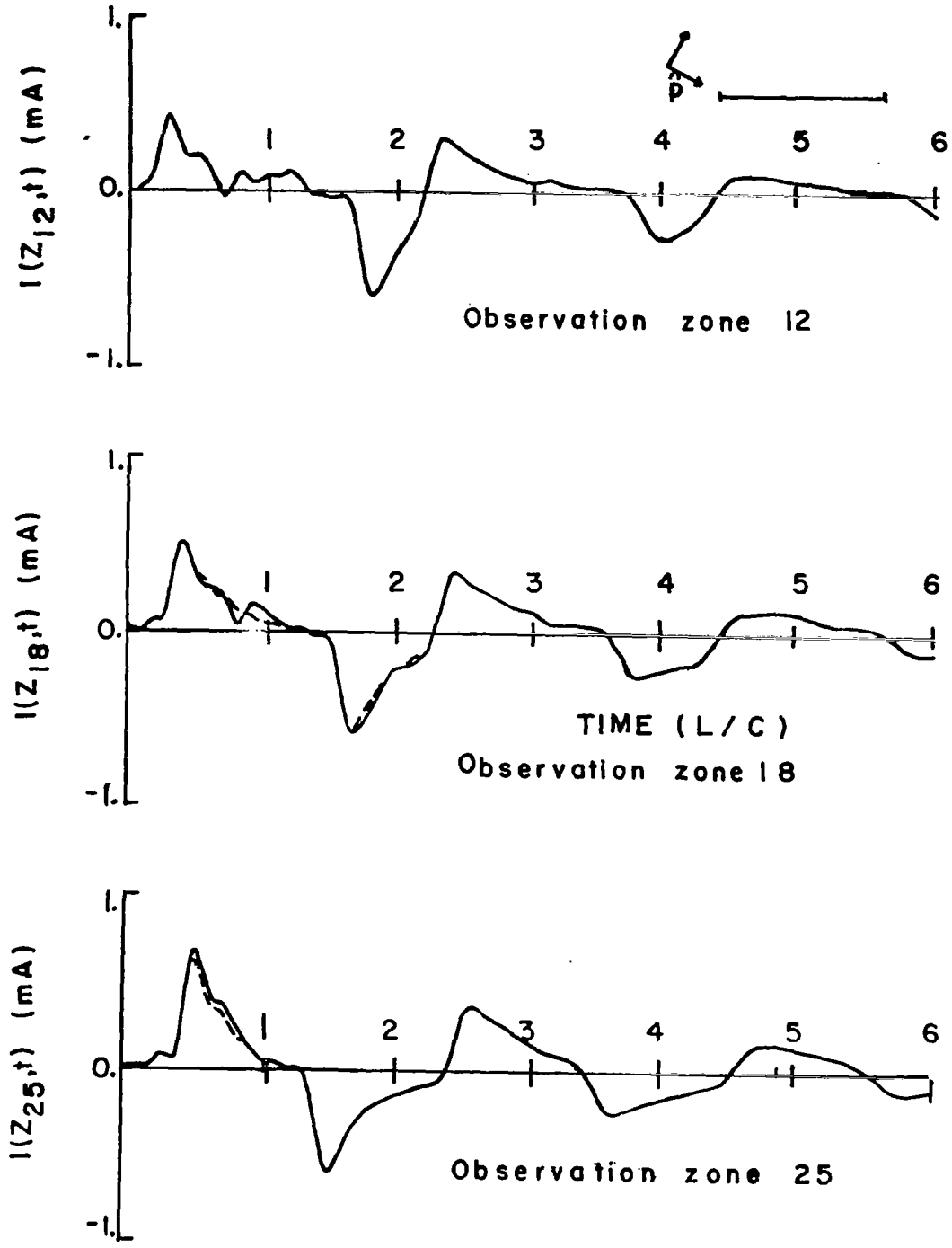

Figure 21. Transient currents for a plane wave with a double exponential time history at 60 degrees incidence. Solid lines are from an expansion of the SEM parameters derived from transient data, and the dashed lines are from an expansion of the SEM parameters obtained from an integral equation technique.

CHAPTER V

CONCLUSIONS

Using the method presented in this document it appears feasible to extract the SEM description from spatially-sampled transient data. To obtain a complete SEM description for a system several data completeness considerations must be taken into account. They are as follows:

- For extraction of the SEM description, the magnitude of the spectrum of the forcing function at the highest frequency of interest must be well above the noise level to insure this frequency gets excited;
- The spatial placement of the generator must be such that all modes of interest are excited; and
- The extrapolation of the SEM description cannot be carried out if the expansion extends beyond the band limitations of the description, or if the excitation couples data which were not coupled in the data from which the description is derived.

The quality of data extracted is directly dependent on the quality of the transient responses. For center-excitation conditions the coupling is a maximum for even modes, and the resulting SEM description was very favorable. For off-center excitation the coupling is not as strong, therefore the results were weaker than for a center excitation. In general, we observe that the information content of the original data is transformable to the SEM form.

Results of the extrapolation to different excitations were favorable. This proved true even when clearly discernable errors were present in the

extracted SEM data. This is due to the fact that the excitation spectrum in the extrapolation gave relatively low weighting to the higher order resonances where the errors were evident. One would not expect to be able to apply a spectrum which gave dominant weighting to resonances which were weakly coupled in the source data.

The ultimate applicability of this method to practical situations, and, in particular, measured data depends on a noise tolerant pole extractor. While some of the recent developments such as the sliding-window scheme offer promise, more work is in order in this direction. For the present purpose, further consideration should be given to exploitation of the spatial redundancy present in the data.

REFERENCES

1. Baum, C. E., "The Singularity Expansion Method," Ch. 3 of Transient Electromagnetic Fields, L. B. Felsen ed., Springer-Verlag, Heidelberg, 1976.

2. Baum, C. E., "On the Singularity Expansion Method for the Solution of Electromagnetic Interaction Problems," Interaction Note 88, December 11, 1971.

3. Mittra, R. and Van Blaricum, M. L., "A Novel Technique for Extracting the SEM Poles and Residues of a System Directly from its Transient Response," 1974 Annual URSI Meeting, University of Colorado, Boulder, Colorado, October 14-17, 1974.

4. Van Blaricum, M. L. and Mittra, R., "Techniques for the Extension and Generalization of Prony's Method," 1975 Annual URSI Meeting, University of Colorado, Boulder, Colorado, October 20-23, 1975.

5. Van Blaricum, M. L. and Mittra, R., "A Technique for Extracting the Poles and Residues of a System Directly from its Transient Response," IEEE Trans. Antennas Propagat., Vol. AP-23, No. 6, pp. 777-781, Nov. 1975, and also Interaction Note 245, February 1975.

6. Van Blaricum, M. L. and Mittra, R., "Techniques for Extracting the Complex Resonances of a System Directly from its Transient Response," Air Force Weapons Laboratory Report No. 76-250, Air Force Weapons Laboratory, Kirtland Air Force Base, NM, April, 1977, and also Interaction Note 301, December 1975.

7. Dudley, D. G., "Random Errors in Prony's Method," USNC/URSI 1976 Annual Meeting, Amherst, Ma, October, 1976. Also as: "Parametric Modeling of Transient Electromagnetic Systems," Radio Science, to be published.

8. Lager, D. L., Hudson, H. G., Poggio, A. J., Miller, E. K., and Deadrick, F. J., "Prony's Method for Time Domain," Mini-Symposium on Modal Analysis of Experimental Data, Albuquerque, NM, March, 1977.

9. Van Blaricum, M. L., "Bibliography," Mini-Symposium on Modal Analysis of Experimental Data," Albuquerque, NM, March, 1977.

10. Poggio, A. J., Van Blaricum, M. L., Miller, E. K., Mittra, R., "Evaluation of a Processing Technique for Transient Data," IEEE Trans. Antennas Propagat., Vol. AP-26, No. 1, pp. 165-171, Jan. 1978.

11. Pearson, L. and Mittra, R., "The Singularity Expansion Representation of the Transient Electromagnetic Coupling through a Rectangular Aperature," Electromagnetics Laboratory Report No. 76-7, University of Illinois, Urbana, Ill., June, 1976, and also Interaction Note 296, June 1976.

12. Pearson, L. W. and Mittra, R., "Casuality Considerations in SEM Coupling Coefficient Forms," 1976 APS International Symposium, Amherst, Mass., October, 1976.

13. Van Blaricum, M. L., "A Numerical Technique for the Time-Dependent Solution of Thin-Wire Structures with Multiple Junctions," Electromagnetics Laboratory Report 73-15, University of Illinois, Urbana, Illinois, December, 1973.

14. Tesche, F. M., "Application of the Singularity Expansion Method to the Analysis of Impedance Loaded Linear Antennas," Sensor and Simulator Note 177, Air Force Weapons Laboratory, May, 1973.